

1 **Differential response of digesta- and mucosa-associated intestinal microbiota to**  
2 **dietary black soldier fly (*Hermetia illucens*) larvae meal in seawater phase Atlantic**  
3 **salmon (*Salmo salar*)**

4  
5 Yanxian Li<sup>1\*</sup>, Leonardo Bruni<sup>2</sup>, Alexander Jaramillo-Torres<sup>1</sup>, Karina Gajardo<sup>1,3</sup>,

6 Trond M. Kortner<sup>1</sup>, Åshild Krogdahl<sup>1</sup>

7  
8 <sup>1</sup>Department of Paraclinical Sciences, Faculty of Veterinary Medicine, Norwegian  
9 University of Life Sciences, Oslo, Norway.

10 <sup>2</sup>Department of Agriculture, Food, Environment and Forestry, University of Florence,  
11 Firenze, Italy.

12 <sup>3</sup>Biomar AS, Trondheim, Norway

13  
14 Running title: Response of salmon gut flora to dietary insect meal

15  
16 \*Address correspondence to Yanxian Li, [yanxian.li@nmbu.no](mailto:yanxian.li@nmbu.no)

17  
18 Yanxian Li and Leonardo Bruni contributed equally to this work. Author order was  
19 selected based on CRediT (Contributor Roles Taxonomy).

20 **Abstract**

21 **Background:** Intestinal digesta is commonly used for studying responses of microbiota  
22 to dietary shifts, yet evidence is accumulating that it represents an incomplete view of  
23 the intestinal microbiota. The present work aims to investigate the differences between  
24 digesta- and mucosa-associated intestinal microbiota in Atlantic salmon (*Salmo salar*)  
25 and how they may respond differently to dietary perturbations. In a 16-week seawater  
26 feeding trial, Atlantic salmon were fed either a commercially-relevant reference diet or  
27 an insect meal diet containing ~15% black soldier fly (*Hermetia illucens*) larvae meal.  
28 The digesta- and mucosa-associated distal intestinal microbiota were profiled by 16S  
29 rRNA gene sequencing.

30 **Results:** Regardless of diet, we observed substantial differences between digesta- and  
31 mucosa-associated intestinal microbiota. Microbial richness and diversity were much  
32 higher in the digesta than the mucosa. The insect meal diet altered the distal intestinal  
33 microbiota resulting in higher microbial richness and diversity. The diet effect, however,  
34 depended on the sample origin. Digesta-associated intestinal microbiota showed more  
35 pronounced changes than the mucosa-associated microbiota. Multivariate association  
36 analyses identified two mucosa-enriched taxa, *Brevinema andersonii* and unclassified  
37 *Spirochaetaceae*, associated with the expression of genes related to immune responses  
38 and barrier function in the distal intestine, respectively.

39 **Conclusions:** Our data show that salmon intestinal digesta and mucosa harbor  
40 microbial communities with clear differences. Mucosa-associated intestinal microbiota  
41 seems more resilient to variations in the diet composition than digesta-associated

42 intestinal microbiota. To fully unveil the response of intestinal microbiota to dietary  
43 changes, concurrent profiling of digesta- and mucosa-associated intestinal microbiota  
44 is recommended whenever feasible.

45

46 **Keywords:** Atlantic salmon, Diet, Black soldier fly, Microbiota, Digesta, Mucosa

## 47 **Background**

48 The global population is projected to reach 9.7 billion in 2050 [1], requiring an increase  
49 in the food supply by 25-70% [2]. Producing more safe and high-quality food in a  
50 sustainable way to meet the global population growth is a great challenge for our  
51 generation. Fish are considered as nutritionally valuable part of the human diet and play  
52 an important role in the global food supply [3, 4]. The average annual growth rate of  
53 world food fish consumption in the period 2019-2030 is projected to be 1.4 percent,  
54 reaching 28 million tonnes live weight in 2030 [5]. Atlantic salmon (*Salmo salar*) is the  
55 most produced marine fish species and one of the most economically important farmed  
56 fish worldwide [6]. While Atlantic salmon are strictly carnivorous in the wild, farmed  
57 Atlantic salmon have experienced a substantial shift in the diet composition due to a  
58 limited supply of marine ingredients. Marine ingredients used for Norwegian farmed  
59 Atlantic salmon have gradually been replaced by plant sources, decreasing from ~90% in  
60 1990 to ~25% in 2016 [7]. Due to concerns on the economic, environmental and social  
61 sustainability of the current raw materials for Atlantic salmon farming [6], more  
62 sustainable alternative feed ingredients, such as insects [8] and yeasts [9], have been  
63 developed and used.

64 It is now well established that intestinal microbiota plays a pivotal role in host  
65 development and physiology, from being an essential element for the development of  
66 normal gut functions and immunity [10, 11] to modulating lipid metabolism and energy  
67 balance [12, 13]. In salmonid aquaculture, microbial-related products such as probiotics

68 and prebiotics have been successfully applied to improve the robustness of fish during  
69 stress and disease [14]. Recent advances in sequencing technologies have transformed  
70 our ability to study the composition and dynamics of fish intestinal microbiota, leading  
71 to increasing interest in selective manipulation of intestinal microbiota. Diet is one of the  
72 key factors in shaping the intestinal microbiota. While long-term dietary habits have a  
73 considerable effect on the structure and activity of host intestinal microbiota [15-17],  
74 short-term dietary change also alters the intestinal microbiota in a rapid and reproducible  
75 way [18]. Different dietary components selectively promote or suppress the growth of  
76 certain microbial clades, which in turn could inflict important effects on the host health  
77 and disease resistance [19, 20]. The use of alternative feed ingredients may not only affect  
78 the nutrient utilization, fish growth, health, welfare and product quality, but also intestinal  
79 microbiota in Atlantic salmon [21-23]. While studies in mammals and fish have revealed  
80 substantial differences between the digesta- and mucosa-associated intestinal microbiota  
81 [21, 24-27], most studies investigating diet effects on the intestinal microbiota of fish  
82 have sampled the digesta only or a mixture of digesta and mucosa. Evidence is  
83 accumulating that digesta- and mucosa-associated intestinal microbiota in fish respond  
84 differently to dietary changes [21, 28-31]. Profiling only one of or a mixture of digesta-  
85 and mucosa-associated microbiota may obscure the response of intestinal microbiota to  
86 dietary changes.

87 Characterizing intestinal microbiota and its associations with host responses is an  
88 essential step towards identifying key microbial clades promoting fish health and welfare.  
89 Ultimately, a milestone in the fish microbiota research would be knowing how to

90 selectively manipulate the microbiota to improve the growth performance, disease  
91 resistance and health status of farmed fish. The main aims of the present study were (i) to  
92 compare distal intestinal microbiota of Atlantic salmon fed a commercially relevant diet  
93 or an insect meal diet, (ii) to further explore the dissimilarity between digesta- and  
94 mucosa-associated microbiota and the differences in their response to dietary changes,  
95 and (iii) to identify associations between microbial clades and host responses. This work  
96 was part of a larger study consisting of a freshwater and seawater feeding trial that aimed  
97 to investigate the nutritional value and possible health effects for Atlantic salmon of a  
98 protein-rich insect meal produced from black soldier fly (*Hermetia illucens*) larvae. The  
99 results presented herein focuses on the intestinal microbiota in seawater phase Atlantic  
100 salmon fed an insect meal diet containing ~15% black soldier fly larvae meal for 16 weeks.  
101 Results on the feed utilization, growth performance, fillet quality, intestinal  
102 histopathology and gene expression have been reported elsewhere [32-34]. In brief, there  
103 was lack of evidence that the insect meal diet negatively affected the feed utilization,  
104 growth performance or fillet quality of Atlantic salmon. Profiling of genes related to lipid  
105 metabolism, immune responses, barrier functions and stress responses in the proximal  
106 and distal intestine showed little evidence of diet effect. Histopathological examination  
107 of intestinal segments showed enterocyte steatosis in the proximal and mid intestine in  
108 both diet groups, but it was less severe in the proximal intestine of fish fed the insect meal  
109 diet.

## 110 **Results**

111 Hereafter, different sample groups are named based on the combination of diet (REF vs.  
112 IM) and sample origin (DID vs. DIM). Hence, in addition to the extraction blanks, library  
113 blanks and mock, we have four different sample types, i.e., REF-DID, REF-DIM, IM-  
114 DID and IM-DIM.

### 115 **qPCR**

116 Since C<sub>q</sub> values of most mucosa DNA templates were out of the linear range of the  
117 standard curve, the raw C<sub>q</sub> value was used as a proxy of 16S rRNA gene quantity in the  
118 diluted DNA templates (Figure S1). On average, REF-DID showed the highest 16S rRNA  
119 gene quantities (mean C<sub>q</sub> = 24.7), followed by the mocks (mean C<sub>q</sub> = 26.1) and IM-DID  
120 (mean C<sub>q</sub> = 28.4). Irrespective of diet, mucosa DNA templates (REF-DIM, IM-DIM)  
121 showed similar 16S rRNA gene quantities (mean C<sub>q</sub> = 30) that were close to extraction  
122 blanks (mean C<sub>q</sub> = 32.4).

### 123 **Taxonomic composition**

124 All the eight bacterial species included in the mock were successfully identified at genus  
125 level with *E. faecalis*, *L. fermentum*, *L. monocytogenes* and *S. aureus* further being  
126 annotated at the species level (Figure S2A). At the genus level, the average Pearson's *r*  
127 between the expected and observed taxonomic profile of the mock was 0.33, whereas the  
128 Pearson's *r* between the observed taxonomic profile of the mock was 0.98. The relative  
129 abundance of most Gram-positive bacteria, *L. monocytogenes* and *E. faecalis* in particular,  
130 were underestimated. In contrast, the relative abundance of Gram-negative bacteria was

---

131 overestimated. Most ASVs (97.5% - 99.9%) in the extraction and library blanks were  
132 classified as *Pseudomonas* (Figure S2B), which was the main contaminating taxon  
133 removed from the biological samples along with other contaminants including  
134 *Curtobacterium*, *Jeotgalicoccus*, *Modestobacter*, *Cutibacterium*, *Hymenobacter*,  
135 *Brevundimonas*, *Micrococcus*, *Sphingomonas*, *Devosia*, *Sphingomonas aurantiaca* and  
136 *Marinobacter adhaerens*. The exact sequence of the contaminating ASVs and their  
137 relative abundance in the extraction and library blanks are available in Table S1.

138 The taxonomic composition of mucosa samples showed higher similarity than that of  
139 the digesta samples, which were more diet-dependent (Figure 1). At the phylum level, the  
140 dominant taxa of mucosa samples for both diets were *Spirochaetes* (REF-DIM, 72 ±  
141 34.6 %; IM-DIM, 47 ± 35.2 %) (mean ± S.D.), *Proteobacteria* (REF-DIM, 21 ± 34.1 %;  
142 IM-DIM, 23 ± 34.1 %), *Firmicutes* (REF-DIM, 1 ± 2.8 %; IM-DIM, 11 ± 13.5 %),  
143 *Tenericutes* (REF-DIM, 4 ± 8 %; IM-DIM, 8 ± 18.8 %) and *Actinobacteria* (REF-DIM,  
144 1 ± 3.4 %; IM-DIM, 9 ± 8.7 %). For digesta samples, the dominant taxa of REF-DID  
145 were *Tenericutes* (33 ± 23.1 %), *Proteobacteria* (31 ± 29.9 %), *Firmicutes* (25 ± 21.1 %)  
146 and *Spirochaetes* (9 ± 12.9 %), whereas IM-DID was dominated by *Firmicutes* (45 ±  
147 16.9 %), *Actinobacteria* (25 ± 9.5 %), *Proteobacteria* (17 ± 27.8 %), *Tenericutes* (7 ±  
148 8.8 %) and *RsaHF231* (4 ± 1.5 %) (Figure 1A). At the genus level, the dominant taxa of  
149 mucosa samples for both diets were *Brevinema* (REF-DIM, 52 ± 40.1 %; IM-DIM, 25 ±  
150 35 %), unclassified *Spirochaetaceae* (REF-DIM, 20 ± 31.8 %; IM-DIM, 22 ± 31.4 %),  
151 *Aliivibrio* (REF-DIM, 18 ± 33.5 %; IM-DIM, 18 ± 35.3 %) and *Mycoplasma* (REF-DIM,  
152 4 ± 8 %; IM-DIM, 8 ± 18.8 %). For digesta samples, the dominant taxa of REF-DID were

---

153 *Mycoplasma* ( $33 \pm 23.1$  %), *Aliivibrio* ( $20 \pm 32.3$  %), *Photobacterium* ( $10 \pm 12.6$  %),  
154 *Brevinema* ( $6 \pm 12.5$  %) and *Lactobacillus* ( $5 \pm 4$  %), whereas IM-DID was dominated  
155 by *Aliivibrio* ( $15 \pm 28.2$  %), unclassified *Lactobacillales* ( $14 \pm 6$  %), *Corynebacterium 1*  
156 ( $13 \pm 5$  %), *Bacillus* ( $8 \pm 3.4$  %), *Mycoplasma* ( $7 \pm 8.8$  %) and *Actinomyces* ( $5 \pm 2$  %)  
157 (Figure 1B).

### 158 **Core microbiota**

159 In total, 108 taxa were identified as core microbiota based on their prevalence in each  
160 sample type (Figure 2; Table S2). Specifically, *Aliivibrio*, *Brevinema andersonii*, and  
161 *Mycoplasma* were identified as core microbiota for all the sample types, the latter two  
162 being universally present in all the samples. Additionally, ten taxa were identified as core  
163 microbiota for digesta samples (REF-DID and IM-DID), which included *Bacillus*,  
164 *Corynebacterium 1*, *Lactobacillus* (*L. aviaries*, *L. fermentum* and two unclassified  
165 species), *Leuconostoc*, *Parageobacillus toebii*, *Ureibacillus* and *Weissella*. No additional  
166 core microbiota taxa were identified for the mucosa samples (REF-DIM and IM-DIM).  
167 *Actinomyces*, *Corynebacterium 1*, *Corynebacterium aurimucosum* ATCC 70097,  
168 *Microbacterium* and unclassified *RsaHF23* were the additional core microbiota taxa  
169 identified for fish fed the insect meal diet (IM-DID and IM-DIM), whereas no additional  
170 core microbiota taxa were identified for fish fed the reference diet (REF-DID and REF-  
171 DIM). Lastly, 86 taxa were found to be more prevalent in IM-DID than in any other  
172 sample type.

### 173 **Alpha-diversity**

174 Regardless of diet, all the alpha-diversity indices were higher in digesta samples than

175 mucosa samples ( $p < 0.05$ ) (Figure 3). Independent of sample origin, all the alpha-  
176 diversity indices were higher in fish fed the IM diet than those fed the REF diet ( $p < 0.05$ ).  
177 A significant interaction between the diet and sample origin effect was detected for the  
178 observed species ( $p = 0.031$ ) and Faith's phylogenetic diversity ( $p = 0.002$ ), both of which  
179 showed a stronger diet effect in digesta samples than mucosa samples.

## 180 **Beta-diversity**

181 The PCoA plots built on the Jaccard and unweighted UniFrac distance matrix showed  
182 clear separations of samples belonging to different dietary groups and sample origins  
183 (Figure 4A-B). However, the average distance between samples from different dietary  
184 groups was dependent on sample origin. Specifically, mucosa samples from different  
185 dietary groups formed clusters close to each other, whereas digesta samples from different  
186 dietary groups were far apart. The PCoA plots built on the Aitchison and PHILR  
187 transformed Euclidean distance matrix also showed separations of samples belonging to  
188 different dietary groups and sample origins (Figure 4C-D). Again, the average distance  
189 between samples from different dietary groups was dependent on sample origin. Mucosa  
190 samples from different dietary groups formed clusters boarding (Figure 4C) or  
191 overlapping (Figure 4D) each other, whereas digesta samples from different dietary  
192 groups were more clearly separated.

193 The PERMANOVA and its following conditional contrasts largely confirmed the PCoA  
194 results. Regardless of the distance matrix used, both main factors had significant effects  
195 on the beta-diversity and their interaction was significant as well ( $p < 0.05$ ) (Table 1).  
196 Results on the tests of homogeneity of multivariate dispersions are shown in Table 2. For

197 Jaccard distance, significant differences in the multivariate dispersions were observed  
198 between digesta and mucosa samples for both diets (REF-DID VS. REF-DIM,  $p = 0.045$ ;  
199 IM-DID VS. IM-DIM,  $p = 0.002$ ), and between diets for digesta samples (REF-DID VS.  
200 IM-DID,  $p = 0.002$ ). For unweighted UniFrac distance, IM-DID showed lower  
201 multivariate dispersions than other sample types resulting in significant differences  
202 compared to REF-DID ( $p = 0.002$ ) and IM-DIM ( $p = 0.002$ ). For Aitchison distance, REF-  
203 DIM showed lower multivariate dispersions than other sample types resulting in  
204 significant differences compared to REF-DID ( $p = 0.046$ ) and IM-DIM ( $p = 0.046$ ). For  
205 PHILR transformed Euclidean distance, the differences in the multivariate dispersions  
206 among the sample types were not significant ( $p > 0.05$ ).

### 207 **Significant associations between microbial clades and sample metadata**

208 The multivariate association analysis identified 53 taxa showing significant associations  
209 with the metadata of interest (Figure 5A). The diagnostic plots showing the raw data  
210 underlying the significant associations are shown in Figures S3-8. Forty-seven  
211 differentially abundant taxa were identified for the sample origin effect, 45 of which,  
212 including *Bacillus*, *Enterococcus*, *Flavobacterium*, *Lactobacillus*, *Lactococcus*,  
213 *Leuconostoc*, *Mycoplasma*, *Peptostreptococcus*, *Photobacterium*, *Staphylococcus*,  
214 *Streptococcus*, *Vagococcus* and *Weissella*, showed lower relative abundances in the  
215 mucosa than the digesta (Figure S3). In contrast, two taxa belonging to the *Spirochaetes*  
216 phylum, *B. andersonii* and unclassified *Spirochaetaceae*, were enriched in the mucosa  
217 (Figure 5B). Thirty-six differentially abundant taxa were identified for the diet effect, 26  
218 of which showed increased relative abundances in fish fed the IM diet (Figure S4).

219 Among these 26 taxa, some were enriched in both intestinal digesta and mucosa which  
220 included *Actinomyces*, unclassified *Bacillaceae*, *Bacillus*, unclassified *Beutenbergiaceae*,  
221 *Brevibacterium*, *Corynebacterium* 1, *Enterococcus*, unclassified *Lactobacillales*,  
222 *Microbacterium*, *Oceanobacillus* and unclassified *RsaHF231* (partially illustrated as  
223 Figure 5C). For the histological scores, the relative abundance of unclassified  
224 *Sphingobacteriaceae* and unclassified *RsaHF231* were found to increase and decrease,  
225 respectively, in fish scored abnormal regarding lamina propria cellularity (lpc) in distal  
226 intestine (Figure S5). The relative abundance of *Acinetobacter* and *Pseudomonas* were  
227 negatively correlated with the distal intestine somatic index (DISI) (Figure S6). Six taxa,  
228 including *Actinomyces*, *B. andersonii*, *Kurthia*, *Lysobacter*, *Microbacterium* and the  
229 unclassified *Sphingobacteriaceae*, were found to associate with the expression of genes  
230 related to immune responses (Figure S7). Notably, the relative abundance of *B. andersonii*  
231 showed a clear positive correlation with the expression levels of immune genes (Figure  
232 5D), which decreased as the PC1 of the PCA increased. Furthermore, 3 taxa including  
233 *Cellulosimicrobium*, *Glutamicibacter* and the unclassified *Spirochaetaceae* were found  
234 to associate with the expression of genes related to barrier functions (Figure S8). The  
235 relative abundance of the unclassified *Spirochaetaceae* showed a negative correlation  
236 with the expression levels of barrier function relevant genes (Figure 5E), which decreased  
237 as the PC1 of the PCA increased.

238 **Discussion**

239 **Core microbiota**

240 In accordance with previous studies in Atlantic salmon [22, 35-40], *Aliivibrio*, *B.*  
241 *andersonii* and *Mycoplasma* were identified as core microbiota in the present study.  
242 *Aliivibrio* is commonly found in the seawater phase Atlantic salmon intestine [37-39, 41-  
243 45] and has been identified as a core taxon of both wild and captive Atlantic salmon [36,  
244 38, 39]. Provided its common presence in seawater, *Aliivibrio* may have originated from  
245 the surrounding water and colonized the intestinal mucosa as Atlantic salmon constantly  
246 drink seawater to prevent dehydration in a hyperosmotic environment. Currently, the  
247 taxon *Aliivibrio* comprises of four closely related species including *Aliivibrio fischeri*,  
248 *Aliivibrio logei*, *Aliivibrio salmonicida* and *Aliivibrio wodanis*, which were split from the  
249 *Vibrio* genus and reclassified as *Aliivibrio* in 2007 [46]. Strains of *A. fischeri* and *A. logei*  
250 have been described as bioluminescent symbionts of certain fishes and squids [47],  
251 whereas *A. salmonicida* and *A. wodanis* have been identified as pathogens for Atlantic  
252 salmon causing cold-water vibriosis [48] and ‘winter ulcer’ [49], respectively.

253 Though *Spirochaetes* has typically been found in low abundances in the Atlantic  
254 salmon intestine [21, 25, 29, 41, 50], two recent studies have identified *B. andersonii* as  
255 a core taxon of both digesta- and mucosa-associated intestinal microbiota in seawater  
256 phase Atlantic salmon [37, 38]. Notably, *B. andersonii* is also a predominant taxon in the  
257 digesta and mucosa in one of the studies [38]. *B. andersonii* was initially isolated from  
258 short-tailed shrews (*Blarina brevicauda*) and white-footed mice (*Peromyscus leucopus*)  
259 as an infectious pathogen [51]. This taxon has also been found in the intestine and gill

260 tissue of rainbow trout (*Oncorhynchus mykiss*) [52], and intestinal digesta of Senegalese  
261 sole (*Solea senegalensis*)[53].

262 *Mycoplasma* is widely distributed in nature and well known for its minute size and lack  
263 of cell wall. It seems to be particularly well-adapted to Atlantic salmon intestine [54].  
264 Like *Aliivibrio*, it has been frequently identified as a core taxon of both wild and captive  
265 Atlantic salmon [22, 35, 37-40]. Notably, it was found to be more abundant in marine  
266 adults than in freshwater juvenile Atlantic salmon [39] and sporadically predominate  
267 intestinal microbial community in the digesta [22, 38, 39, 43, 55] and mucosa [37]  
268 reaching > 90% of total reads in extreme cases. Due to its small compact genome and  
269 limited biosynthesis capacities, *Mycoplasma* typically forms obligate parasitic or  
270 commensal relationships with its host to obtain necessary nutrients such as amino acids,  
271 fatty acids and sterols [56]. Recent shotgun-metagenomic sequencing of the Atlantic  
272 salmon *Mycoplasma* revealed that it is closely related to *Mycoplasma penetrans* [22, 57].  
273 It was suggested that the presence of riboflavin encoding genes and lack of pathogenicity  
274 factors in the metagenome-assembled *Mycoplasma* genome is indicative of a symbiotic  
275 relationship between the *Mycoplasma* and Atlantic salmon [57].

## 276 **Sample origin effect**

277 In line with previous findings in mammals and fish [21, 24-27], we observed substantial  
278 differences between digesta- and mucosa-associated microbiota. The microbial richness  
279 and diversity were much higher in the digesta than the mucosa, as previously observed in  
280 seawater phase Atlantic salmon [21, 25, 38]. Furthermore, most of the bacterial taxa in  
281 the distal intestine, including those commonly found in the Atlantic salmon intestine such

282 as *Bacillus*, *Enterococcus*, *Flavobacterium*, *Lactobacillus*, *Lactococcus*, *Leuconostoc*,  
283 *Mycoplasma*, *Peptostreptococcus*, *Photobacterium*, *Staphylococcus*, *Streptococcus*,  
284 *Vagococcus* and *Weissella*, were less abundant in the mucosa than in the digesta. These  
285 results are suggestive of a selection pressure from the host that determines which  
286 microbial clades colonize and flourish in the intestinal mucus layer [58]. In this study,  
287 two taxa belonging to the *Spirochaetes* phylum, *B. andersonii* and unclassified  
288 *Spirochaetaceae*, were more abundant in the distal intestine mucosa than the digesta. As  
289 aforementioned, *Spirochaetes* were typically found in low abundances in the Atlantic  
290 salmon intestine. Yet a recent study also showed that irrespective of diets *B. andersonii*  
291 seemed to be more abundant in the intestinal mucosa than the digesta of seawater phase  
292 Atlantic salmon [38]. Known for high motility and chemotactic attraction to mucin, some  
293 *Spirochaetes* can penetrate the mucus and associate with the intestinal mucosa [59-61].  
294 Further work is required to confirm whether these taxa are consistently enriched in the  
295 intestinal mucus layer of seawater phase Atlantic salmon.

## 296 **Diet effect**

297 Diet is one of the key factors in shaping the fish intestinal microbiota. In agreement with  
298 previous findings in rainbow trout [31, 62, 63] and laying hens [64, 65], we found that  
299 the insect meal diet altered the distal intestinal microbiota assemblage resulting in higher  
300 microbial richness and diversity. Our findings, showing that the insect meal diet increased  
301 the relative abundance of *Actinomyces*, *Bacillus*, *Brevibacterium*, *Corynebacterium 1* and  
302 *Enterococcus*, are in accord with recent studies in rainbow trout fed diets containing 30%  
303 black soldier fly larvae meal [31, 63]. Importantly, these results were partly confirmed in

304 other studies employing fluorescence *in situ* hybridization for targeted profiling of  
305 changes in the intestinal microbiota. Specifically, increased absolute abundance of  
306 *Lactobacillus/Enterococcus* was found in rainbow trout fed 20% dietary black soldier fly  
307 larvae meal [66], whereas increased absolute abundance of *Bacillus*, *Enterococcus* and  
308 *Lactobacillus* was documented in Siberian sturgeon (*Acipenser baerii*) fed 15% black  
309 soldier fly larvae meal [67].

310 The increases in the relative abundance of specific microbial clades in Atlantic salmon  
311 fed the insect meal diet may be explained by feed-borne microbiota and/or feed  
312 composition. Bacterial taxa, including *Actinomyces*, *Bacillus*, *Brevibacterium*,  
313 *Corynebacterium*, *Enterococcus*, *Oceanobacillus* and *RsaHF231*, have been found in  
314 black soldier fly whole larvae or larvae intestine [68-71]. The fact that *RsaHF231* has not  
315 been documented in fish before indicates that these bacterial taxa may have partially  
316 originated from black soldier fly larvae meal. Our results from the freshwater feeding trial  
317 showed that these bacterial taxa were also enriched in the intestinal digesta and mucosa  
318 of Atlantic salmon smolts fed an insect meal diet containing 60% soldier fly larvae meal.  
319 Importantly, these bacterial taxa were also detected in the feed pellets which contained  
320 considerable amount of bacterial DNA (unpublished data). Given the hydrothermal  
321 treatments the feed pellets underwent during the extrusion, the feed-borne microbiota  
322 profiled by the DNA sequencing techniques could have largely originated from dead  
323 bacteria and bacterial spores rather than living bacteria. As sequencing-based methods  
324 cannot differentiate between living and dead cells, future studies should investigate to  
325 what extent the feed-borne microbiota may contribute to, or confound the observed diet

326 effects on intestinal microbiota, using methods that distinguish living and dead bacteria  
327 such as viability PCR and RNA sequencing [72]. On the other hand, unique nutrients in  
328 the insect meal diet such as chitin, an essential component of the insect exoskeleton, may  
329 have selectively promoted the growth of certain intestinal microbes. Many bacterial  
330 species belonging to *Bacillus* can produce chitinase [73]. *Bacillus* and *Lactobacillus* were  
331 two of the predominant taxa in the intestinal mucosa of Atlantic salmon fed a 5% chitin  
332 diet, the former of which displayed the highest *in vitro* chitinase activity [74].

### 333 **Significant interactions between diet and sample origin effect**

334 We observed in the present study that the diet effect on the intestinal microbial community  
335 richness and structure was dependent on the sample origin, with mucosa-associated  
336 intestinal microbiota showing higher resilience to the dietary change. Our results  
337 corroborate previous findings in rainbow trout revealing that mucosa-associated intestinal  
338 microbiota was less influenced by dietary inclusion of 30% black soldier fly larvae meal  
339 compared to digesta-associated intestinal microbiota [30, 31]. Results from molecular-  
340 based studies on salmonid intestinal microbiota hitherto suggest that diet modulates  
341 digesta- and mucosa-associated intestinal microbiota to varying degrees with the latter  
342 generally being more resilient to dietary interventions [21, 28-31, 37]. As such, current  
343 practices of profiling only one of or a mixture of digesta- and mucosa-associated  
344 microbiota may obscure the response of intestinal microbiota to dietary changes. To fully  
345 unveil the response of intestinal microbiota to dietary changes, we recommend concurrent  
346 profiling of digesta- and mucosa-associated intestinal microbiota whenever it is feasible.

347 **Significant associations between microbial clades and sample metadata**

348 To our knowledge, only a few studies have carried out association analysis between  
349 intestinal microbial clades and host responses in Atlantic salmon. As such, our results  
350 should be treated as preliminary observations and critically evaluated in later studies.  
351 Herein, we highlight the significant associations between two mucosa-enriched taxa and  
352 host gene expressions in the intestine. Specifically, *B. andersonii*, part of the core  
353 microbiota, was associated with the expression of genes related to pro- and anti-  
354 inflammatory responses whereas the unclassified *Spirochaetaceae* was associated with  
355 the expression of genes related to barrier function. Intestinal microbiota is well known to  
356 modulate the local immune responses and intestinal epithelial barrier function [75].  
357 Furthermore, it is hypothesized that mucosa-associated microbiota plays a more crucial  
358 role in shaping the host immunity in that it can interact both directly and indirectly with  
359 intestinal epithelial barrier whereas digesta-associated microbiota can only interact  
360 indirectly [58]. Taken together, further research should be undertaken to investigate the  
361 potential ecological and functional significance of these two taxa for seawater phase  
362 Atlantic salmon.

363 **Quality control: use of mock and negative controls**

364 As in any field of research, conducting a well-controlled microbiome study requires great  
365 care in the experiment design such as setting up appropriate experimental controls. The  
366 use of mock as a positive control allows for critical evaluation and optimization of  
367 microbiota profiling workflow. That all the bacterial taxa in the mock were correctly  
368 identified at the genus level indicates that the current workflow is reliable for the

369 taxonomic profiling of intestinal microbiota. Furthermore, the taxonomic profile of mock  
370 from different DNA extraction batches was fairly similar, suggesting that the results  
371 generated by the current workflow are also largely reproducible. However, the low  
372 concordance between the expected and observed relative abundance of bacterial taxa in  
373 the mock is reminiscent of the fact that bias is introduced at different steps of the marker-  
374 gene survey [76-78], among which DNA extraction and PCR amplification are the two  
375 largest sources of bias due to preferential extraction and amplification of some microbial  
376 clades over others. In line with previous observations that Gram-positive bacteria may be  
377 more subjective to incomplete lysis during DNA extraction due to their tough cell walls  
378 [79, 80], the recovery of most Gram-positive bacteria in the mock was lower than the  
379 expected. The insufficient lysing of Gram-positive bacteria in the mock was largely  
380 mitigated in our later experiments by using a mixture of beads with different sizes for the  
381 bead beating during DNA extraction (unpublished data). The bias in the marker-gene  
382 sequencing experiments, as reflected in the observed taxonomic profile of the mock,  
383 highlights the necessity of validating such results by absolute quantification techniques  
384 such as cultivation (if possible), qPCR, flow cytometry and fluorescence *in situ*  
385 hybridization.

386 Reagent contamination is a common issue in molecular-based studies of microbial  
387 communities. The main contaminating taxon identified in this study is *Pseudomonas*,  
388 which has been reported as a common reagent contaminant in numerous studies [81-87].  
389 Given the dominance of *Pseudomonas* in the negative controls of both DNA extraction  
390 and PCR, most of the observed contamination has likely derived from PCR reagents such

391 as molecular-grade water [88-90]. Notably, *Pseudomonas* has also been isolated from  
392 intestinal digesta and mucosa of Atlantic salmon by traditional culturing approaches [74,  
393 91-93], and reported as a member of Atlantic salmon core microbiota in culture-  
394 independent studies [21, 25, 35, 36, 40, 94]. Due to the low taxonomic resolution of  
395 amplicon sequencing, it is difficult to discern contaminating taxa from true signals solely  
396 based on taxonomic labels. The inclusion of negative controls, coupled with  
397 quantifications of microbial DNA concentration in the samples, has enabled fast and  
398 reliable identification of contaminating taxa in this study. Besides *Pseudomonas*, other  
399 common reagent contaminants, including *Bradyrhizobium*, *Burkholderia*, *Comamonas*,  
400 *Methylobacterium*, *Propionibacterium*, *Ralstonia*, *Sphingomonas* and *Stenotrophomonas*  
401 [86, 88, 90, 95-99], have also been frequently reported as members of Atlantic salmon  
402 intestinal microbiota, indicating that existing studies of Atlantic salmon intestinal  
403 microbiota may have been plagued with reagent contamination that is hard to ascertain  
404 due to lack of negative controls. As reagent contamination is unavoidable, study-specific  
405 and can critically influence sequencing-based microbiome analyses [88, 100, 101],  
406 negative controls should always be included and sequenced in microbiome studies  
407 especially when dealing with low microbial biomass samples like intestinal mucosa.

## 408 **Conclusions**

409 In summary, we confirmed previous findings in mammals and fish that intestinal digesta  
410 and mucosa harbor microbial communities with clear differences. Regardless of diet,  
411 microbial richness and diversity were much higher in the digesta than the mucosa. The

412 insect meal diet altered the distal intestinal microbiota assemblage resulting in higher  
413 microbial richness and diversity. The diet effect was however dependent on the sample  
414 origin, with mucosa-associated intestinal microbiota being more resilient to the dietary  
415 change. To fully unveil the response of intestinal microbiota to dietary changes,  
416 concurrent profiling of digesta- and mucosa-associated intestinal microbiota is  
417 recommended whenever feasible. Lastly, we identified two mucosa-enriched taxa,  
418 *Brevinema andersonii* and unclassified *Spirochaetaceae*, which were associated with the  
419 expression in the distal intestine of genes related to immune responses and barrier  
420 function, respectively. As mucosa-associated microbiota could play a more critical role  
421 in shaping the host metabolism, their potential functional significance for seawater phase  
422 Atlantic salmon merits further investigations.

## 423 **Methods**

### 424 **Experimental fish, diet and sampling**

425 A 16-week seawater feeding trial with Atlantic salmon (initial body weight = 1.40 kg,  
426 S.D. = 0.043 kg) was conducted at the Gildeskål Research Station (GIFAS), Nordland,  
427 Norway. The experimental fish were randomly assigned into 6 adjacent square net pens  
428 (5 x 5 m) with a depth of 5 m, each containing 90 fish. The fish were fed, in triplicate net  
429 pens, either a commercially-relevant reference diet (REF) with a combination of fish meal,  
430 soy protein concentrate, pea protein concentrate, corn gluten and wheat gluten as the  
431 protein source, or an insect meal diet (IM) wherein all the fish meal and most of the pea  
432 protein concentrate were replaced by black soldier fly larvae meal (Protix Biosystems BV,

433 Dongen, The Netherlands). Fish were fed by hand until apparent satiation once or twice  
434 daily depending on the duration of daylight. During the feeding trial, the water  
435 temperature ranged from 7 °C to 13 °C. Further details on the formulation and chemical  
436 composition of the diets, and insect meal have been reported elsewhere [33, 34].

437 At the termination of the feeding trial, the average body weight of fish reached 3.7 kg.  
438 Six fish were randomly taken from each net pen, anesthetized with tricaine  
439 methanesulfonate (MS222®; Argent Chemical Laboratories, Redmond, WA, USA) and  
440 euthanized by a sharp blow to the head. After cleaning the exterior of each fish with 70%  
441 ethanol, the distal intestine, i.e., the segment from the increase in intestinal diameter and  
442 the appearance of transverse luminal folds to the anus, was aseptically removed from the  
443 abdominal cavity, placed in a sterile Petri dish and opened longitudinally. Only fish with  
444 digesta along the whole intestine were sampled to ensure that the intestine had been  
445 exposed to the diets. The intestinal digesta was collected into a 50 mL skirted sterile  
446 centrifuge tube and mixed thoroughly using a spatula. An aliquot of the homogenate was  
447 then transferred into a 1.5 mL sterile Eppendorf tube and snap-frozen in liquid N<sub>2</sub> for the  
448 profiling of digesta-associated intestinal microbiota. A tissue section from the mid part of  
449 the distal intestine was excised and rinsed in sterile phosphate-buffered saline 3 times to  
450 remove traces of the remaining digesta. After rinsing, the intestinal tissue was  
451 longitudinally cut into 3 pieces for histological evaluation (fixed in 4% phosphate-  
452 buffered formaldehyde solution for 24 h and transferred to 70% ethanol for storage), RNA  
453 extraction (preserved in RNAlater solution and stored at -20 °C) and profiling of mucosa-  
454 associated intestinal microbiota (snap-frozen in liquid N<sub>2</sub>), respectively. The collection

455 of microbiota samples was performed near a gas burner to secure aseptic conditions. After  
456 the sampling of each fish, tools were cleaned and decontaminated by a 70% ethanol spray  
457 and flaming. Microbiota samples of the distal intestine digesta (DID) and mucosa (DIM)  
458 were transported in dry ice and stored at -80 °C until DNA extraction.

#### 459 **DNA extraction**

460 Total DNA was extracted from ~200 mg distal intestine digesta or mucosa using the  
461 QIAamp<sup>®</sup> DNA Stool Mini Kit (Qiagen, Hilden, Germany; catalog no., 51504) with some  
462 modifications to the manufacturer's specifications as described before [21], except that 2  
463 mL prefilled bead tubes (Qiagen; catalog no., 13118-50) were used for the bead beating.  
464 For quality control purposes, a companion "blank extraction" sample was added to each  
465 batch of sample DNA extraction by omitting the input material, whereas an additional  
466 microbial community standard (ZymoBIOMICS™, Zymo Research, California, USA;  
467 catalog no., D6300), i.e. mock, was included for each DNA extraction kit as a positive  
468 control. The mock consists of 8 bacteria (*Pseudomonas aeruginosa*, *Escherichia coli*,  
469 *Salmonella enterica*, *Lactobacillus fermentum*, *Enterococcus faecalis*, *Staphylococcus*  
470 *aureus*, *Listeria monocytogenes*, *Bacillus subtilis*) and 2 yeasts (*Saccharomyces*  
471 *cerevisiae*, *Cryptococcus neoformans*).

#### 472 **Amplicon PCR**

473 The V1-2 hypervariable regions of the bacterial 16S rRNA gene were amplified using the  
474 primer set 27F (5'-AGA GTT TGA TCM TGG CTC AG-3') and 338R (5'-GCW GCC  
475 WCC CGT AGG WGT-3') [102]. The PCR was run in a total reaction volume of 25 µL  
476 containing 12.5 µL of Phusion<sup>®</sup> High-Fidelity PCR Master Mix (Thermo Scientific, CA,

477 USA; catalog no., F531L), 10.9  $\mu$ L molecular grade H<sub>2</sub>O, 1  $\mu$ L DNA template and 0.3  $\mu$ L  
478 of each primer (10  $\mu$ M). The amplification program was set as follows: initial  
479 denaturation at 98 °C for 3 min; 35 cycles of denaturation at 98 °C for 15 s, annealing  
480 decreasing from 63 °C to 53 °C in 10 cycles for 30 s followed by 25 cycles at 53 °C for  
481 30 s, and extension at 72 °C for 30 s; followed by a final extension at 72 °C for 10 min.  
482 For samples with faint or invisible bands in the agarose gel after PCR, the PCR condition  
483 was optimized by applying serial dilutions to the DNA templates to reduce the influence  
484 of PCR inhibitors. All the digesta samples were diluted 1:2 in buffer ATE (10 mM Tris-  
485 Cl, pH 8.3, with 0.1 mM EDTA and 0.04% NaN<sub>3</sub>) whereas all the mucosa samples were  
486 diluted 1:32. The formal amplicon PCR was run in duplicate incorporating two negative  
487 PCR controls, which were generated by replacing the template DNA with molecular grade  
488 H<sub>2</sub>O. The duplicate PCR products were then pooled and examined by a 1.5% agarose gel  
489 electrophoresis.

#### 490 **Quantification of 16S rRNA gene by qPCR**

491 To assist in identifying contaminating sequences, the 16S rRNA gene quantity in the  
492 diluted DNA templates used for the amplicon PCR was measured by qPCR. The qPCR  
493 assays were performed using a universal primer set (forward, 5'-CCA TGA AGT CGG  
494 AAT CGC TAG-3'; reverse, 5'-GCT TGA CGG GCG GTG T-3') that has been used for  
495 bacterial DNA quantification in previous studies [103, 104]. The assays were carried out  
496 using the LightCycler 96 (Roche Applied Science, Basel, Switzerland) in a 10  $\mu$ L reaction  
497 volume, which contained 2  $\mu$ L of PCR-grade water, 1  $\mu$ L diluted DNA template, 5  $\mu$ L  
498 LightCycler 480 SYBR Green I Master Mix (Roche Applied Science) and 1  $\mu$ L (3  $\mu$ M)

499 of each primer. Samples, together with the extraction blanks and mock, were run in  
500 duplicate in addition to Femto™ bacterial DNA standards (Zymo Research; catalog no.,  
501 E2006) and a no-template control of the qPCR assay. The qPCR program encompassed  
502 an initial enzyme activation step at 95 °C for 2 min, 45 three-step cycles of 95 °C for 10  
503 s, 60 °C for 30 s and 72 °C for 15 s, and a melting curve analysis at the end.  
504 Quantification cycle (Cq) values were determined using the second derivative method  
505 [105]. The specificity of qPCR amplification was confirmed by evaluating the melting  
506 curve of qPCR products and the band pattern on the agarose gel after electrophoresis.  
507 The inter-plate calibration factor was calculated following the method described in  
508 [106], using the bacterial DNA standards as inter-plate calibrators.

## 509 **Sequencing**

510 The sequencing was carried out on a Miseq platform following the Illumina 16S  
511 metagenomic sequencing library preparation protocol [107]. Briefly, the PCR products  
512 were cleaned using the Agencourt AMPure XP system (Beckman Coulter, Indiana, USA;  
513 catalog no., A63881), multiplexed by dual indexing using the Nextera XT Index Kit  
514 (Illumina, California, USA; catalog no., FC-131-1096) and purified again using the  
515 AMPure beads. After the second clean-up, representative libraries were selected and  
516 analyzed using the Agilent DNA 1000 Kit (Agilent Technologies, California, USA;  
517 catalog no., 5067-1505) to verify the library size. Cleaned libraries were quantified using  
518 the Invitrogen Qubit™ dsDNA HS Assay Kit (Thermo Fisher Scientific, California, USA;  
519 catalog no., Q32854), diluted to 4 nM in 10 mM Tris (pH 8.5) and finally pooled in an  
520 equal volume. Negative controls with library concentrations lower than 4 nM were pooled

521 in equal volume directly. Due to the low diversity of amplicon library, 15% Illumina  
522 generated PhiX control (catalog no., FC-110-3001) was spiked in by combining 510  $\mu$ L  
523 amplicon library with 90  $\mu$ L PhiX control library. The library was loaded at 6 pM and  
524 sequenced using the Miseq Reagent Kit v3 (600-cycle) (Illumina; catalog no., MS-102-  
525 3003).

## 526 **Sequence data processing**

527 The raw sequence data were processed by the DADA2 1.14 in R 3.6.3 [108] to infer  
528 amplicon sequence variants (ASVs) [109]. Specifically, the demultiplexed paired-ended  
529 reads were trimmed off the primer sequences (forward reads, first 20 bps; reverse reads,  
530 first 18 bps), truncated at the position where the median Phred quality score crashed  
531 (forward reads, at position 290 bp; reverse reads, at position 248 bp) and filtered off low-  
532 quality reads. After trimming and filtering, the run-specific error rates were estimated and  
533 the ASVs were inferred by pooling reads from all the samples sequenced in the same run.  
534 The chimeras were removed using the “pooled” method after merging the reads. The  
535 resulting raw ASV table and representative sequences were imported into QIIME2  
536 (version, 2020.2) [110]. The taxonomy was assigned by a scikit-learn naive Bayes  
537 machine-learning classifier [111], which was trained on the SILVA 132 99% OTUs [112]  
538 that were trimmed to only include the regions of 16S rRNA gene amplified by our primers.  
539 Taxa identified as chloroplasts or mitochondria were excluded from the ASV table. The  
540 ASV table was conservatively filtered to remove ASVs that had no phylum-level  
541 taxonomic assignment or appeared in only one biological sample. Contaminating ASVs  
542 were identified based on two suggested criteria: contaminants are often found in negative

543 controls and inversely correlate with sample DNA concentration [87]. The ASVs filtered  
544 from the raw ASV table were also removed from the representative sequences, which  
545 were then inserted into a reference phylogenetic tree built on the SILVA 128 database  
546 using SEPP [113]. The alpha rarefaction curves and the core metrics results were  
547 generated with a sampling depth of 10000 and 2047 sequences per sample, respectively.  
548 For downstream data analysis and visualization, QIIME2 artifacts were imported into R  
549 using the *qiime2R* package [114] and a *phyloseq* [115] object was assembled from the  
550 sample metadata, ASV table, taxonomy and phylogenetic tree. The core microbiota and  
551 alpha-diversity indices were computed using the ASV table collapsed at the species level.  
552 The core microbiota was calculated based on the 80% prevalence threshold and visualized  
553 by the Venn's diagram. The alpha-diversity indices, including observed species, Pielou's  
554 evenness, Shannon's index and Faith's phylogenetic diversity (PD), were computed via  
555 the R packages *microbiome* [116] and *picante* [117]. For beta-diversity analyses, we used  
556 distance matrices including Jaccard distance, unweighted UniFrac distance, Aitchison  
557 distance and phylogenetic isometric log-ratio (PHILR) transformed Euclidean distance.  
558 Since rarefying remains to be the best solution for unweighted distance matrices [118],  
559 the Jaccard distance and unweighted UniFrac distance were computed in QIIME2 using  
560 the rarefied ASV table. The compositionality-aware distance matrices, Aitchison distance  
561 and PHILR transformed Euclidean distance, were calculated using the unrarefied ASV  
562 table. The Aitchison distance was computed by the *DEICODE* plugin in QIIME2, a form  
563 of Aitchison distance that is robust to high levels of sparsity by using the matrix  
564 completion to handle the excessive zeros in the microbiome data [119]. The PHILR

565 transform of the ASV table was performed in R using the *philr* package [120]. The  
566 selected distance matrices were explored and visualized by the principal coordinates  
567 analysis (PCoA).

## 568 **Multivariate association analysis**

569 The ASV table was collapsed at the genus level before running the multivariate  
570 association analysis. Bacterial taxa of very low abundance (< 0.01%) or low prevalence  
571 (present in < 25% of samples) were removed from the feature table. The microbial clades  
572 were then tested for significant associations with metadata of interest by MaAsLin2  
573 (version, 0.99.12) (<https://huttenhower.sph.harvard.edu/maaslin2>) in R, using the default  
574 parameters. The results of the analysis are the associations of specific microbial clades  
575 with metadata, deconfounding the influence of other factors included in the model.  
576 Association was considered significant when the *q*-value was below 0.25. Metadata  
577 included in the multivariate association testing are fixed factors Diet + Sample origin +  
578 distal intestine somatic index (DISI) + lamina propria cellularity (histological scores) +  
579 immune response (qPCR) + barrier function (qPCR), and random factors FishID +  
580 NetPen. FishID was nested in NetPen, and NetPen nested in Diet. Lamina propria  
581 cellularity reflects the severity of inflammation in the distal intestine. Based on the degree  
582 of cellular infiltration within the lamina propria, a value of normal, mild, moderate,  
583 marked or severe was assigned. To make the data appropriate for the association testing,  
584 the highly skewed five-category scores were collapsed into more balanced binary data,  
585 i.e., normal and abnormal. The immune-related genes included for the association testing  
586 were myeloid differentiation factor 88 (*myd88*), interleukin 1 $\beta$  (*il1 $\beta$* ), interleukin 8 (*il8*),

587 cluster of differentiation 3  $\gamma\delta$  (*cd3 $\gamma\delta$* ), transforming growth factor  $\beta$ 1 (*tgf $\beta$ 1*), interferon  $\gamma$   
588 (*ifn $\gamma$* ), interleukin 17A (*il17a*), fork-head box P3 (*foxp3*) and interleukin 10 (*il10*), whose  
589 expression levels were higher in the distal intestine of fish assigned abnormal regarding  
590 lamina propria cellularity. Since the expression levels of immune-related genes were  
591 highly correlated, we ran a principal component analysis (PCA) and extracted the first  
592 principle component (PC1) for the association testing to avoid multicollinearity and  
593 reduce the number of association testing. For genes relevant to the barrier function, which  
594 included claudin-15 (*cldn15*), claudin-25b (*cldn25b*), zonula occludens 1 (*zol*), E-  
595 cadherin / cadherin 1 (*cdh1*) and mucin-2 (*muc2*), we also used the PC1 of the PCA for  
596 the association testing based on the same considerations.

## 597 **Statistics**

598 All the statistical analyses were run in R except for the PERMANOVA, which was run  
599 in PRIMER v7. The differences in the alpha-diversity indices were compared using linear  
600 mixed-effects models via the *lme4* package [121]. Predictor variables in the models  
601 included the fixed effects Diet + Sample origin + Diet x Sample origin, and the random  
602 effects FishID + NetPen. The models were validated by visual inspections of residual  
603 diagnostic plots generated by the *ggResidpanel* package [122]. The statistical significance  
604 of fixed predictors was estimated by Type III ANOVA with Kenward-Roger's  
605 approximation of denominator degrees of freedom via the *lmerTest* package [123]. When  
606 the interaction between the main effects was significant, conditional contrasts for the main  
607 effects were made via the *emmeans* package [124]. To compare the differences in beta-  
608 diversity, we performed the PERMANOVA [125] using the same predictors included in

609 the linear mixed-effects models. Terms with negative estimates for components of  
610 variation were sequentially removed from the model via term pooling, starting with the  
611 one showing the smallest mean squares. At each step, the model was reassessed whether  
612 more terms needed to be removed or not. Conditional contrasts for the main effects were  
613 constructed when their interaction was significant. Monte Carlo  $p$  values were computed  
614 as well when the unique permutations for the terms in the PERMANOVA were small ( $<$   
615 100). The homogeneity of multivariate dispersions among groups was visually assessed  
616 with boxplots and was formally tested by the permutation test, PERMDISP [126], via the  
617 R package *vegan* [127]. Multiple comparisons were adjusted by the Benjamini-Hochberg  
618 procedure where applicable. Differences were regarded as significant when  $p < 0.05$ .

## 619 **Declarations**

## 620 **Acknowledgments**

621 The authors wish to thank Ellen K. Hage for organizing the sampling and technicians at  
622 the GIFAS for their committed animal care and supports during the sampling.

## 623 **Authors' contributions**

624 TMK and ÅK conceptualized and designed the study. YL, LB and KG participated in the  
625 sample collection. YL, LB and AJ-T carried out the laboratory works. YL performed the  
626 bioinformatics, statistical analyses and data visualization. YL and LB completed the first  
627 draft of the manuscript. All the authors read, revised and approved the final version of the  
628 manuscript.

629 **Funding**

630 YL was granted a scholarship from the China Scholarship Council to pursue his PhD  
631 degree at Norwegian University of Life Sciences. This work was a spin-off of the  
632 “AquaFly” project (grant number, 238997), funded by the Research Council of Norway  
633 and managed by the Institute of Marine Research. Costs related to this study were covered  
634 by Norwegian University of Life Sciences. The funding agencies had no role in study  
635 design, data collection and interpretation, decision to publish or preparation of the  
636 manuscript.

637 **Availability of data and materials**

638 The raw 16S rRNA gene sequencing data are deposited at the NCBI SRA database under  
639 the BioProject PRJNA555355. Other raw data and code for reproducing our results are  
640 available from the GitHub repository ([https://github.com/yanxian/Li\\_AqF12-](https://github.com/yanxian/Li_AqF12-Microbiota_ASM_2020)  
641 [Microbiota\\_ASM\\_2020](https://github.com/yanxian/Li_AqF12-Microbiota_ASM_2020)).

642 **Ethics approval and consent to participate**

643 The experiment was conducted in compliance with the Norwegian Animal Welfare Act  
644 10/07/2009 and the EU Directive on the Protection of Animals used for Scientific  
645 Purposes (2010/63/EU).

646 **Consent for publication**

647 Not applicable.

648 **Competing interests**

649 The authors declare that they have no competing interests.

---

## 650 Reference

- 651 1. United Nations. World population prospects 2019: Highlights.  
652 <https://population.un.org/wpp/Publications/>
- 653 2. Hunter MC, Smith RG, Schipanski ME, Atwood LW, Mortensen DA. Agriculture in 2050:  
654 recalibrating targets for sustainable intensification. *Bioscience*. 2017;67:386-391.
- 655 3. Tacon AGJ, Metian M. Fish matters: importance of aquatic foods in human nutrition and global  
656 food supply. *Rev Fish Sci*. 2013;21:22-38.
- 657 4. Khalili Tilami S, Sampels S. Nutritional value of fish: lipids, proteins, vitamins, and minerals. *Rev*  
658 *Fish Sci Aquac*. 2018;26:243-253.
- 659 5. FAO: The State of World Fisheries and Aquaculture. Rome, Italy: FAO; 2020.
- 660 6. FAO: The State of World Fisheries and Aquaculture. Rome, Italy: FAO; 2018.
- 661 7. Aas TS, Ytrestøyl T, Åsgård T. Utilization of feed resources in the production of Atlantic salmon  
662 (*Salmo salar*) in Norway: An update for 2016. *Aquac Rep*. 2019;15:100216.
- 663 8. Sánchez-Muros M-J, Barroso FG, Manzano-Agugliaro F. Insect meal as renewable source of food  
664 for animal feeding: a review. *J Clean Prod*. 2014;65:16-27.
- 665 9. Øverland M, Skrede A. Yeast derived from lignocellulosic biomass as a sustainable feed resource  
666 for use in aquaculture. *J Sci Food Agric*. 2016;97:733-742.
- 667 10. Bates JM, Mittge E, Kuhlman J, Baden KN, Cheesman SE, Guillemin K. Distinct signals from the  
668 microbiota promote different aspects of zebrafish gut differentiation. *Dev Biol*. 2006;297:374-386.
- 669 11. Rawls JF, Samuel BS, Gordon JI. Gnotobiotic zebrafish reveal evolutionarily conserved responses  
670 to the gut microbiota. *Proc Natl Acad Sci U S A*. 2004;101:4596-4601.
- 671 12. Falcinelli S, Picchietti S, Rodiles A, Cossignani L, Merrifield DL, Taddei AR, Maradonna F,  
672 Olivotto I, Gioacchini G, Carnevali O. *Lactobacillus rhamnosus* lowers zebrafish lipid content by  
673 changing gut microbiota and host transcription of genes involved in lipid metabolism. *Sci Rep*.  
674 2015;5:9336.
- 675 13. Semova I, Carten JD, Stombaugh J, Mackey LC, Knight R, Farber SA, Rawls JF. Microbiota  
676 regulate intestinal absorption and metabolism of fatty acids in the zebrafish. *Cell Host Microbe*.  
677 2012;12:277-288.
- 678 14. Merrifield DL, Dimitroglou A, Foey A, Davies SJ, Baker RT, Bøgwald J, Castex M, Ringø E. The  
679 current status and future focus of probiotic and prebiotic applications for salmonids. *Aquaculture*.  
680 2010;302:1-18.
- 681 15. Wu GD, Chen J, Hoffmann C, Bittinger K, Chen YY, Keilbaugh SA, Bewtra M, Knights D, Walters  
682 WA, Knight R, et al. Linking long-term dietary patterns with gut microbial enterotypes. *Science*.  
683 2011;334:105-108.
- 684 16. Muegge BD, Kuczynski J, Knights D, Clemente JC, González A, Fontana L, Henrissat B, Knight  
685 R, Gordon JI. Diet drives convergence in gut microbiome functions across mammalian phylogeny  
686 and within humans. *Science*. 2011;332:970-974.
- 687 17. De Filippo C, Cavalieri D, Di Paola M, Ramazzotti M, Poullet JB, Massart S, Collini S, Pieraccini  
688 G, Lionetti P. Impact of diet in shaping gut microbiota revealed by a comparative study in children  
689 from Europe and rural Africa. *Proc Natl Acad Sci U S A*. 2010;107:14691-14696.
- 690 18. David LA, Maurice CF, Carmody RN, Gootenberg DB, Button JE, Wolfe BE, Ling AV, Devlin AS,  
691 Varma Y, Fischbach MA, et al. Diet rapidly and reproducibly alters the human gut microbiome.  
692 *Nature*. 2014;505:559-563.

- 693 19. Wang Z, Klipfell E, Bennett BJ, Koeth R, Levison BS, Dugar B, Feldstein AE, Britt EB, Fu X,  
694 Chung YM, et al. Gut flora metabolism of phosphatidylcholine promotes cardiovascular disease.  
695 Nature. 2011;472:57-63.
- 696 20. Hryckowian AJ, Van Treuren W, Smits SA, Davis NM, Gardner JO, Bouley DM, Sonnenburg JL.  
697 Microbiota-accessible carbohydrates suppress *Clostridium difficile* infection in a murine model.  
698 Nat Microbiol. 2018;3:662-669.
- 699 21. Gajardo K, Jaramillo-Torres A, Kortner TM, Merrifield DL, Tinsley J, Bakke AM, Krogdahl Å.  
700 Alternative protein sources in the diet modulate microbiota and functionality in the distal intestine  
701 of Atlantic salmon (*Salmo salar*). Appl Environ Microbiol. 2017;83:e02615-02616.
- 702 22. Jin Y, Angell IL, Rod Sandve S, Snipen LG, Olsen Y, Rudi K. Atlantic salmon raised with diets  
703 low in long-chain polyunsaturated n-3 fatty acids in freshwater have a *Mycoplasma*-dominated gut  
704 microbiota at sea. Aquac Environ Interact. 2019;11:31-39.
- 705 23. Schmidt V, Amaral-Zettler L, Davidson J, Summerfelt S, Good C. Influence of fishmeal-free diets  
706 on microbial communities in Atlantic salmon (*Salmo salar*) recirculation aquaculture systems.  
707 Appl Environ Microbiol. 2016;82:4470-4481.
- 708 24. Eckburg PB, Bik EM, Bernstein CN, Purdom E, Dethlefsen L, Sargent M, Gill SR, Nelson KE,  
709 Relman DA. Diversity of the human intestinal microbial flora. Science. 2005;308:1635-1638.
- 710 25. Gajardo K, Rodiles A, Kortner TM, Krogdahl Å, Bakke AM, Merrifield DL, Sorum H. A high-  
711 resolution map of the gut microbiota in Atlantic salmon (*Salmo salar*): A basis for comparative  
712 gut microbial research. Sci Rep. 2016;6:30893.
- 713 26. Looft T, Allen HK, Cantarel BL, Levine UY, Bayles DO, Alt DP, Henrissat B, Stanton TB. Bacteria,  
714 phages and pigs: the effects of in-feed antibiotics on the microbiome at different gut locations.  
715 ISME J. 2014;8:1566.
- 716 27. Lyons PP, Turnbull JF, Dawson KA, Crumlish M. Exploring the microbial diversity of the distal  
717 intestinal lumen and mucosa of farmed rainbow trout *Oncorhynchus mykiss* (Walbaum) using next  
718 generation sequencing (NGS). Aquac Res. 2017;48:77-91.
- 719 28. Huyben D, Sun L, Moccia R, Kiessling A, Dicksved J, Lundh T. Dietary live yeast and increased  
720 water temperature influence the gut microbiota of rainbow trout. J Appl Microbiol.  
721 2018;124:1377-1392.
- 722 29. Jaramillo-Torres A, Rawling MD, Rodiles A, Mikalsen HE, Johansen LH, Tinsley J, Forberg T,  
723 Aasum E, Castex M, Merrifield DL. Influence of Dietary Supplementation of Probiotic  
724 *Pediococcus acidilactici* MA18/5M During the Transition From Freshwater to Seawater on  
725 Intestinal Health and Microbiota of Atlantic Salmon (*Salmo salar* L.). Front Microbiol.  
726 2019;10:2243.
- 727 30. Rimoldi S, Gini E, Iannini F, Gasco L, Terova G. The Effects of Dietary Insect Meal from *Hermetia*  
728 *illucens* Prepupae on Autochthonous Gut Microbiota of Rainbow Trout (*Oncorhynchus mykiss*).  
729 Animals (Basel). 2019;9.
- 730 31. Terova G, Rimoldi S, Ascione C, Gini E, Ceccotti C, Gasco L. Rainbow trout (*Oncorhynchus*  
731 *mykiss*) gut microbiota is modulated by insect meal from *Hermetia illucens* prepupae in the diet.  
732 Rev Fish Biol Fish. 2019;29:465-486.
- 733 32. Bruni L, Belghit I, Lock E-J, Secci G, Taiti C, Parisi G. Total replacement of dietary fish meal  
734 with black soldier fly (*Hermetia illucens*) larvae does not impair physical, chemical or volatile  
735 composition of farmed Atlantic salmon (*Salmo salar* L.). J Sci Food Agric. 2020;100:1038-1047.
- 736 33. Li Y, Kortner TM, Chikwati EM, Belghit I, Lock E-J, Krogdahl Å. Total replacement of fish meal

- 737 with black soldier fly (*Hermetia illucens*) larvae meal does not compromise the gut health of  
738 Atlantic salmon (*Salmo salar*). *Aquaculture*. 2020;520:734967.
- 739 34. Belghit I, Liland NS, Gjesdal P, Biancarosa I, Menchetti E, Li Y, Waagbø R, Krogdahl Å, Lock E-  
740 J. Black soldier fly larvae meal can replace fish meal in diets of sea-water phase Atlantic salmon  
741 (*Salmo salar*). *Aquaculture*. 2019;503:609-619.
- 742 35. Dehler CE, Secombes CJ, Martin SA. Seawater transfer alters the intestinal microbiota profiles of  
743 Atlantic salmon (*Salmo salar* L.). *Sci Rep*. 2017;7:13877.
- 744 36. Dehler CE, Secombes CJ, Martin SAM. Environmental and physiological factors shape the gut  
745 microbiota of Atlantic salmon parr (*Salmo salar* L.). *Aquaculture*. 2017;467:149-157.
- 746 37. Gupta S, Feckaninova A, Lokesh J, Koscova J, Sorensen M, Femandes J, Kiron V. *Lactobacillus*  
747 dominate in the intestine of Atlantic salmon fed dietary probiotics. *Front Microbiol*. 2019;9.
- 748 38. Gupta S, Lokesh J, Abdelhafiz Y, Siriyappagounder P, Pierre R, Sorensen M, Fernandes JMO, Kiron  
749 V. Macroalga-derived alginate oligosaccharide alters intestinal bacteria of Atlantic salmon. *Front*  
750 *Microbiol*. 2019;10.
- 751 39. Llewellyn MS, McGinnity P, Dionne M, Letourneau J, Thonier F, Carvalho GR, Creer S, Derome  
752 N. The biogeography of the Atlantic salmon (*Salmo salar*) gut microbiome. *ISME J*.  
753 2015;10:1280-1284.
- 754 40. Webster TMU, Consuegra S, Hitchings M, de Leaniz CG. Interpopulation variation in the Atlantic  
755 salmon microbiome reflects environmental and genetic diversity. *Appl Environ Microbiol*.  
756 2018;84:e00691-00618.
- 757 41. Fogarty C, Burgess CM, Cotter PD, Cabrera-Rubio R, Whyte P, Smyth C, Bolton DJ. Diversity  
758 and composition of the gut microbiota of Atlantic salmon (*Salmo salar*) farmed in Irish waters. *J*  
759 *Appl Microbiol*. 2019;127:648-657.
- 760 42. Godoy FA, Miranda CD, Wittwer GD, Aranda CP, Calderon R. High variability of levels of  
761 *Aliivibrio* and lactic acid bacteria in the intestinal microbiota of farmed Atlantic salmon *Salmo*  
762 *salar* L. *Ann Microbiol*. 2015;65:2343-2353.
- 763 43. Karlsen C, Ottem K, Brevik ØJ, Davey M, Sørum H, Winther - Larsen H. The environmental and  
764 host - associated bacterial microbiota of Arctic seawater - farmed Atlantic salmon with ulcerative  
765 disorders. *J Fish Dis*. 2017;40:1645-1663.
- 766 44. Zarkasi KZ, Abell GCJ, Taylor RS, Neuman C, Hatje E, Tamplin ML, Katouli M, Bowman JP.  
767 Pyrosequencing-based characterization of gastrointestinal bacteria of Atlantic salmon (*Salmo*  
768 *salar* L.) within a commercial mariculture system. *J Appl Microbiol*. 2014;117:18-27.
- 769 45. Zarkasi KZ, Taylor RS, Abell GC, Tamplin ML, Glencross BD, Bowman JP. Atlantic salmon  
770 (*Salmo salar* L.) gastrointestinal microbial community dynamics in relation to digesta properties  
771 and diet. *Microb Ecol*. 2016;71:589-603.
- 772 46. Urbanczyk H, Ast JC, Higgins MJ, Carson J, Dunlap PV. Reclassification of *Vibrio fischeri*, *Vibrio*  
773 *logei*, *Vibrio salmonicida* and *Vibrio wodanis* as *Aliivibrio fischeri* gen. nov., comb. nov., *Aliivibrio*  
774 *logei* comb. nov., *Aliivibrio salmonicida* comb. nov. and *Aliivibrio wodanis* comb. nov. *Int J Syst*  
775 *Evol Microbiol*. 2007;57:2823-2829.
- 776 47. Dunlap PV, Ast JC, Kimura S, Fukui A, Yoshino T, Endo H. Phylogenetic analysis of host-  
777 symbiont specificity and codivergence in bioluminescent symbioses. *Cladistics*. 2007;23:507-532.
- 778 48. Egidius E, Wiik R, Andersen K, Hoff K, Hjeltnes B. *Vibrio salmonicida* sp. nov., a new fish  
779 pathogen. *Int J Syst Evol Microbiol*. 1986;36:518-520.
- 780 49. Lunder T, Sørum H, Holstad G, Steigerwalt AG, Mowinckel P, Brenner DJ. Phenotypic and

- 781 genotypic characterization of *Vibrio viscosus* sp. nov. and *Vibrio wodanis* sp. nov. isolated from  
782 Atlantic salmon (*Salmo salar*) with 'winter ulcer'. Int J Syst Evol Microbiol. 2000;50:427-450.
- 783 50. Webster TMU, Rodriguez - Barreto D, Castaldo G, Gough P, Consuegra S, Garcia de Leaniz C.  
784 Environmental plasticity and colonisation history in the Atlantic salmon microbiome: a  
785 translocation experiment. Molecular ecology. 2020;29:886-898.
- 786 51. Anderson JF, Johnson RC, Magnarelli LA, Hyde FW, Andreadis TG. New infectious spirochete  
787 isolated from short-tailed shrews and white-footed mice. J Clin Microbiol. 1987;25:1490-1494.
- 788 52. Brown RM, Wiens GD, Salinas I. Analysis of the gut and gill microbiome of resistant and  
789 susceptible lines of rainbow trout (*Oncorhynchus mykiss*). Fish Shellfish Immunol. 2019;86:497-  
790 506.
- 791 53. Tapia-Paniagua S, Vidal S, Lobo C, Prieto-Álamo M, Jurado J, Cordero H, Cerezuela R, de la  
792 Banda IG, Esteban M, Balebona M. The treatment with the probiotic *Shewanella putrefaciens*  
793 Pdp11 of specimens of *Solea senegalensis* exposed to high stocking densities to enhance their  
794 resistance to disease. Fish Shellfish Immunol. 2014;41:209-221.
- 795 54. Heys C, Cheaib B, Buseti A, Kazlauskaitė R, Maier L, Sloan WT, Ijaz UZ, Kaufmann J,  
796 McGinnity P, Llewellyn MS. Neutral processes dominate microbial community assembly in  
797 Atlantic salmon, *Salmo salar*. Appl Environ Microbiol. 2020;86.
- 798 55. Holben W, Williams P, Saarinen M, Särkilahti L, Apajalahti J. Phylogenetic analysis of intestinal  
799 microflora indicates a novel *Mycoplasma* phylotype in farmed and wild salmon. Microb Ecol.  
800 2002;44:175-185.
- 801 56. Razin S, Yogev D, Naot Y. Molecular biology and pathogenicity of mycoplasmas. Microbiol Mol  
802 Biol Rev. 1998;62:1094-1156.
- 803 57. Cheaib B, Yang P, Kazlauskaitė R, Lindsay E, Heys C, De Noa M, Schaal P, Dwyer T, Sloan W,  
804 Ijaz UZ, Llewellyn MS. Unpicking the mysterious symbiosis of *Mycoplasma* in salmonids.  
805 Preprint at <https://www.biorxiv.org/content/10.1101/2020.07.17.209767v1>. 2020.
- 806 58. Van den Abbeele P, Van de Wiele T, Verstraete W, Possemiers S. The host selects mucosal and  
807 luminal associations of coevolved gut microorganisms: a novel concept. FEMS Microbiol Rev.  
808 2011;35:681-704.
- 809 59. Kennedy M, Rosnick D, Ulrich R, Yancey Jr R. Association of *Treponema hyodysenteriae* with  
810 porcine intestinal mucosa. J Gen Microbiol. 1988;134:1565-1576.
- 811 60. Milner J, Sellwood R. Chemotactic response to mucin by *Serpulina hyodysenteriae* and other  
812 porcine spirochetes: potential role in intestinal colonization. Infect Immun. 1994;62:4095-4099.
- 813 61. Witters NA, Duhamel GE: Motility-regulated mucin association of *Serpulina pilosicoli*, the agent  
814 of colonic spirochetosis of humans and animals. In *Advances in Experimental Medicine and*  
815 *Biology. Volume 473*: Springer; 1999: 199-205
- 816 62. Bruni L, Pastorelli R, Viti C, Gasco L, Parisi G. Characterisation of the intestinal microbial  
817 communities of rainbow trout (*Oncorhynchus mykiss*) fed with *Hermetia illucens* (black soldier  
818 fly) partially defatted larva meal as partial dietary protein source. Aquaculture. 2018;487:56-63.
- 819 63. Huyben D, Vidaković A, Hallgren SW, Langeland M. High-throughput sequencing of gut  
820 microbiota in rainbow trout (*Oncorhynchus mykiss*) fed larval and pre-pupae stages of black  
821 soldier fly (*Hermetia illucens*). Aquaculture. 2019;500:485-491.
- 822 64. Borrelli L, Coretti L, Dipineto L, Bovera F, Menna F, Chiariotti L, Nizza A, Lembo F, Fioretti A.  
823 Insect-based diet, a promising nutritional source, modulates gut microbiota composition and  
824 SCFAs production in laying hens. Sci Rep. 2017;7:1-11.

- 825 65. Kawasaki K, Hashimoto Y, Hori A, Kawasaki T, Hirayasu H, Iwase S, Hashizume A, Ido A, Miura  
826 C, Miura T, et al. Evaluation of black soldier fly (*Hermetia illucens*) larvae and pre-pupae raised  
827 on household organic waste, as potential ingredients for poultry feed. *Animals (Basel)*. 2019;9.
- 828 66. Jozefiak A, Nogales-Merida S, Mikolajczak Z, Rawski M, Kieronczyk B, Mazurkiewicz J. The  
829 utilization of full-fat insect meal in rainbow trout (*Oncorhynchus mykiss*) nutrition: The effects on  
830 growth performance, intestinal microbiota and gastrointestinal tract histomorphology. *Ann Anim  
831 Sci*. 2019;19:747-765.
- 832 67. Jozefiak A, Nogales-Merida S, Rawski M, Kieronczyk B, Mazurkiewicz J. Effects of insect diets  
833 on the gastrointestinal tract health and growth performance of Siberian sturgeon (*Acipenser baerii*  
834 Brandt, 1869). *BMC Microbiol*. 2019;15.
- 835 68. Jiang CL, Jin WZ, Tao XH, Zhang Q, Zhu J, Feng SY, Xu XH, Li HY, Wang ZH, Zhang ZJ. Black  
836 soldier fly larvae (*Hermetia illucens*) strengthen the metabolic function of food waste  
837 biodegradation by gut microbiome. *Microb Biotechnol*. 2019;12:528-543.
- 838 69. Bruno D, Bonelli M, De Filippis F, Di Lelio I, Tettamanti G, Casartelli M, Ercolini D, Caccia S.  
839 The intestinal microbiota of *Hermetia illucens* larvae is affected by diet and shows a diverse  
840 composition in the different midgut regions. *Appl Environ Microbiol*. 2019;85:e01864-01818.
- 841 70. Wynants E, Froominckx L, Crauwels S, Verreth C, De Smet J, Sandrock C, Wohlfahrt J, Van Schelt  
842 J, Depraetere S, Lievens B. Assessing the microbiota of black soldier fly larvae (*Hermetia illucens*)  
843 reared on organic waste streams on four different locations at laboratory and large scale. *Microb  
844 Ecol*. 2019;77:913-930.
- 845 71. Zheng L, Crippen TL, Singh B, Tarone AM, Dowd S, Yu Z, Wood TK, Tomberlin JK. A survey of  
846 bacterial diversity from successive life stages of black soldier fly (Diptera: Stratiomyidae) by using  
847 16S rDNA pyrosequencing. *J Med Entomol*. 2013;50:647-658.
- 848 72. Emerson JB, Adams RI, Roman CMB, Brooks B, Coil DA, Dahlhausen K, Ganz HH, Hartmann  
849 EM, Hsu T, Justice NB, et al. Schrodinger's microbes: Tools for distinguishing the living from the  
850 dead in microbial ecosystems. *Microbiome*. 2017;5:86.
- 851 73. Cody R. Distribution of chitinase and chitobiase in *Bacillus*. *Curr Microbiol*. 1989;19:201-205.
- 852 74. Askarian F, Zhou ZG, Olsen RE, Sperstad S, Ringo E. Culturable autochthonous gut bacteria in  
853 Atlantic salmon (*Salmo salar* L.) fed diets with or without chitin. Characterization by 16S rRNA  
854 gene sequencing, ability to produce enzymes and in vitro growth inhibition of four fish pathogens.  
855 *Aquaculture*. 2012;326:1-8.
- 856 75. Maynard CL, Elson CO, Hatton RD, Weaver CT. Reciprocal interactions of the intestinal  
857 microbiota and immune system. *Nature*. 2012;489:231-241.
- 858 76. McLaren MR, Willis AD, Callahan BJ. Consistent and correctable bias in metagenomic  
859 sequencing experiments. *Elife*. 2019;8.
- 860 77. Brooks JP, Edwards DJ, Harwich MD, Rivera MC, Fettweis JM, Serrano MG, Reris RA, Sheth  
861 NU, Huang B, Girerd P. The truth about metagenomics: quantifying and counteracting bias in 16S  
862 rRNA studies. *BMC Microbiol*. 2015;15:66.
- 863 78. Sinha R, Abnet CC, White O, Knight R, Huttenhower C. The microbiome quality control project:  
864 baseline study design and future directions. *Genome Biol*. 2015;16:276.
- 865 79. Costea PI, Zeller G, Sunagawa S, Pelletier E, Alberti A, Levenez F, Tramontano M, Driessen M,  
866 Hercog R, Jung F-E. Towards standards for human fecal sample processing in metagenomic  
867 studies. *Nat Biotechnol*. 2017;35:1069.
- 868 80. Santiago A, Panda S, Mengels G, Martinez X, Azpiroz F, Dore J, Guarner F, Manichanh C.

- 869 Processing faecal samples: a step forward for standards in microbial community analysis. BMC  
870 Microbiol. 2014;14:112.
- 871 81. Lazarevic V, Gaia N, Girard M, Schrenzel J. Decontamination of 16S rRNA gene amplicon  
872 sequence datasets based on bacterial load assessment by qPCR. BMC Microbiol. 2016;16:73.
- 873 82. Kim D, Hofstaedter CE, Zhao C, Mattei L, Tanes C, Clarke E, Lauder A, Sherrill-Mix S, Chehoud  
874 C, Kelsen J, et al. Optimizing methods and dodging pitfalls in microbiome research. Microbiome.  
875 2017;5:52.
- 876 83. Jousselin E, Clamens AL, Galan M, Bernard M, Maman S, Gschloessl B, Duport G, Meseguer AS,  
877 Calevro F, Coeur d'acier A. Assessment of a 16S rRNA amplicon Illumina sequencing procedure  
878 for studying the microbiome of a symbiont-rich aphid genus. Mol Ecol Resour. 2016;16:628-640.
- 879 84. Jost T, Lacroix C, Braegger C, Chassard C. Assessment of bacterial diversity in breast milk using  
880 culture-dependent and culture-independent approaches. Br J Nutr. 2013;110:1253-1262.
- 881 85. Jervis-Bardy J, Leong LEX, Marri S, Smith RJ, Choo JM, Smith-Vaughan HC, Nosworthy E,  
882 Morris PS, O'Leary S, Rogers GB, Marsh RL. Deriving accurate microbiota profiles from human  
883 samples with low bacterial content through post-sequencing processing of Illumina MiSeq data.  
884 Microbiome. 2015;3:19.
- 885 86. Glassing A, Dowd SE, Galandiuk S, Davis B, Chiodini RJ. Inherent bacterial DNA contamination  
886 of extraction and sequencing reagents may affect interpretation of microbiota in low bacterial  
887 biomass samples. Gut Pathog. 2016;8:24.
- 888 87. Davis NM, Proctor DM, Holmes SP, Relman DA, Callahan BJ. Simple statistical identification  
889 and removal of contaminant sequences in marker-gene and metagenomics data. Microbiome.  
890 2018;6:226.
- 891 88. Salter SJ, Cox MJ, Turek EM, Calus ST, Cookson WO, Moffatt MF, Turner P, Parkhill J, Loman  
892 NJ, Walker AW. Reagent and laboratory contamination can critically impact sequence-based  
893 microbiome analyses. BMC Biol. 2014;12:87.
- 894 89. Kulakov LA, McAlister MB, Ogden KL, Larkin MJ, O'Hanlon JF. Analysis of bacteria  
895 contaminating ultrapure water in industrial systems. Appl Environ Microbiol. 2002;68:1548-1555.
- 896 90. Grahn N, Olofsson M, Ellnebo-Svedlund K, Monstein HJ, Jonasson J. Identification of mixed  
897 bacterial DNA contamination in broad-range PCR amplification of 16S rDNA V1 and V3 variable  
898 regions by pyrosequencing of cloned amplicons. FEMS Microbiol Lett. 2003;219:87-91.
- 899 91. Cantas L, Fraser TWK, Fjellidal PG, Mayer I, Sorum H. The culturable intestinal microbiota of  
900 triploid and diploid juvenile Atlantic salmon (*Salmo salar*) - a comparison of composition and  
901 drug resistance. BMC Vet Res. 2011;7:71.
- 902 92. Navarrete P, Fuentes P, De la Fuente L, Barros L, Magne F, Opazo R, Ibacache C, Espejo R,  
903 Romero J. Short-term effects of dietary soybean meal and lactic acid bacteria on the intestinal  
904 morphology and microbiota of Atlantic salmon (*Salmo salar*). Aquac Nutr. 2013;19:827-836.
- 905 93. Hatje E, Neuman C, Stevenson H, Bowman JP, Katouli M. Population dynamics of *Vibrio* and  
906 *Pseudomonas* species isolated from farmed Tasmanian Atlantic salmon (*Salmo salar* L.): a  
907 seasonal study. Microb Ecol. 2014;68:679-687.
- 908 94. He XP, Chaganti SR, Heath DD. Population-specific responses to interspecific competition in the  
909 gut microbiota of two Atlantic salmon (*Salmo salar*) populations. Microb Ecol. 2018;75:140-151.
- 910 95. Laurence M, Hatzis C, Brash DE. Common contaminants in next-generation sequencing that  
911 hinder discovery of low-abundance microbes. PLoS One. 2014;9:e97876.
- 912 96. Lauder AP, Roche AM, Sherrill-Mix S, Bailey A, Laughlin AL, Bittinger K, Leite R, Elovitz MA,

- 913 Parry S, Bushman FD. Comparison of placenta samples with contamination controls does not  
914 provide evidence for a distinct placenta microbiota. *Microbiome*. 2016;4:29.
- 915 97. Barton HA, Taylor NM, Lubbers BR, Pemberton AC. DNA extraction from low-biomass  
916 carbonate rock: an improved method with reduced contamination and the low-biomass  
917 contaminant database. *J Microbiol Methods*. 2006;66:21-31.
- 918 98. Weyrich LS, Farrer AG, Eisenhofer R, Arriola LA, Young J, Selway CA, Handsley-Davis M, Adler  
919 CJ, Breen J, Cooper A. Laboratory contamination over time during low-biomass sample analysis.  
920 *Mol Ecol Resour*. 2019;19:982-996.
- 921 99. Tanner MA, Goebel BM, Dojka MA, Pace NR. Specific ribosomal DNA sequences from diverse  
922 environmental settings correlate with experimental contaminants. *Appl Environ Microbiol*.  
923 1998;64:3110-3113.
- 924 100. Eisenhofer R, Minich JJ, Marotz C, Cooper A, Knight R, Weyrich LS. Contamination in low  
925 microbial biomass microbiome studies: issues and recommendations. *Trends Microbiol*.  
926 2019;27:105-117.
- 927 101. de Goffau MC, Lager S, Salter SJ, Wagner J, Kronbichler A, Charnock-Jones DS, Peacock SJ,  
928 Smith GCS, Parkhill J. Recognizing the reagent microbiome. *Nat Microbiol*. 2018;3:851-853.
- 929 102. Roeselers G, Mittge EK, Stephens WZ, Parichy DM, Cavanaugh CM, Guillemin K, Rawls JF.  
930 Evidence for a core gut microbiota in the zebrafish. *ISME J*. 2011;5:1595-1608.
- 931 103. Vandeputte D, Kathagen G, D'Hoe K, Vieira-Silva S, Valles-Colomer M, Sabino J, Wang J, Tito  
932 RY, De Commer L, Darzi Y, et al. Quantitative microbiome profiling links gut community  
933 variation to microbial load. *Nature*. 2017;551:507-511.
- 934 104. Ramseier CA, Kinney JS, Herr AE, Braun T, Sugai JV, Shelburne CA, Rayburn LA, Tran HM,  
935 Singh AK, Giannobile WV. Identification of pathogen and host-response markers correlated with  
936 periodontal disease. *J Periodontol*. 2009;80:436-446.
- 937 105. Rasmussen R: Quantification on the LightCycler. In *Rapid cycle real-time PCR*. Springer; 2001:  
938 21-34
- 939 106. Hellemans J, Mortier G, De Paepe A, Speleman F, Vandesompele J. qBase relative quantification  
940 framework and software for management and automated analysis of real-time quantitative PCR  
941 data. *Genome Biol*. 2007;8:R19.
- 942 107. Illumina I. 16S Metagenomic sequencing library preparation. Preparing 16S Ribosomal RNA  
943 Gene Amplicons for the Illumina MiSeq System. 2013:1-28.
- 944 108. R Core Team: R: A language and environment for statistical computing. 2013.
- 945 109. Callahan BJ, McMurdie PJ, Rosen MJ, Han AW, Johnson AJA, Holmes SP. DADA2: high-  
946 resolution sample inference from Illumina amplicon data. *Nat Methods*. 2016;13:581-583.
- 947 110. Bolyen E, Rideout JR, Dillon MR, Bokulich NA, Abnet CC, Al-Ghalith GA, Alexander H, Alm  
948 EJ, Arumugam M, Asnicar F, et al. Reproducible, interactive, scalable and extensible microbiome  
949 data science using QIIME 2. *Nat Biotechnol*. 2019;37:852-857.
- 950 111. Bokulich NA, Kaehler BD, Rideout JR, Dillon M, Bolyen E, Knight R, Huttley GA, Caporaso JG.  
951 Optimizing taxonomic classification of marker-gene amplicon sequences with QIIME 2's q2-  
952 feature-classifier plugin. *Microbiome*. 2018;6:90.
- 953 112. Quast C, Pruesse E, Yilmaz P, Gerken J, Schweer T, Yarza P, Peplies J, Glockner FO. The SILVA  
954 ribosomal RNA gene database project: improved data processing and web-based tools. *Nucleic  
955 Acids Res*. 2013;41:D590-596.
- 956 113. Janssen S, McDonald D, Gonzalez A, Navas-Molina JA, Jiang L, Xu ZZ, Winker K, Kado DM,

- 
- 957 Orwoll E, Manary M. Phylogenetic placement of exact amplicon sequences improves associations  
958 with clinical information. *mSystems*. 2018;3:e00021-00018.
- 959 114. Bisanz JE: qiime2R: Importing QIIME2 artifacts and associated data into R sessions. 2019.
- 960 115. McMurdie PJ, Holmes S. *phyloseq*: an R package for reproducible interactive analysis and  
961 graphics of microbiome census data. 2013.
- 962 116. Lahti L, Shetty S, Blake T, Salojarvi J. *Microbiome r* package. *Tools Microbiome Anal R*. 2017.
- 963 117. Kembel SW, Cowan PD, Helmus MR, Cornwell WK, Morlon H, Ackerly DD, Blomberg SP, Webb  
964 CO. *Picante*: R tools for integrating phylogenies and ecology. *Bioinformatics*. 2010;26:1463-1464.
- 965 118. Weiss S, Xu ZZ, Peddada S, Amir A, Bittinger K, Gonzalez A, Lozupone C, Zaneveld JR,  
966 Vázquez-Baeza Y, Birmingham A. Normalization and microbial differential abundance strategies  
967 depend upon data characteristics. *Microbiome*. 2017;5:27.
- 968 119. Martino C, Morton JT, Marotz CA, Thompson LR, Tripathi A, Knight R, Zengler K. A novel sparse  
969 compositional technique reveals microbial perturbations. *mSystems*. 2019;4:e00016-00019.
- 970 120. Silverman JD, Washburne AD, Mukherjee S, David LA. A phylogenetic transform enhances  
971 analysis of compositional microbiota data. *Elife*. 2017;6:e21887.
- 972 121. Bates D, Mächler M, Bolker B, Walker S. Fitting linear mixed-effects models using *lme4*. *J Stat*  
973 *Softw*. 2015;67:1-48.
- 974 122. Goode K, Rey K: *ggResidpanel*: panels and interactive versions of diagnostic plots using 'ggplot2'.  
975 2019.
- 976 123. Kuznetsova A, Brockhoff PB, Christensen RHB. *lmerTest* package: tests in linear mixed effects  
977 models. *J Stat Softw*. 2017;82.
- 978 124. Lenth R: *emmeans*: estimated marginal means, aka least-squares means. 2019.
- 979 125. Anderson MJ. A new method for non - parametric multivariate analysis of variance. *Austral Ecol*.  
980 2001;26:32-46.
- 981 126. Anderson MJ. Distance - based tests for homogeneity of multivariate dispersions. *Biometrics*.  
982 2006;62:245-253.
- 983 127. Oksanen J, Blanchet FG, Friendly M, Kindt R, Legendre P, McGlinn D, Minchin PR, O'Hara RB,  
984 Simpson GL, Solymos P, et al: *vegan*: Community Ecology Package. 2019.
- 985

986 **Tables**

987 **Table 1. PERMANOVA results and subsequent conditional contrasts.**

Distance matrix	Main effects			Conditional contrasts			
	Diet	Sample origin	Interaction	REF-DID VS. IM-DID	REF-DIM VS. IM-DIM	REF-DID VS. REF-DIM	IM-DID VS. IM-DIM
Jaccard	0.001	0.001	0.001	0.001	0.001	0.001	0.001
Unweighted UniFrac	0.001 <sup>1</sup>	0.001	0.001	0.001 <sup>1</sup>	0.001	0.001	0.001
Aitchison	0.001	0.003	0.004	0.002	0.004	0.004 <sup>1</sup>	0.002 <sup>1</sup>
PHILR (Euclidean) <sup>2</sup>	0.001	0.001	0.001	0.001	0.005	0.001	0.001

988 REF, reference diet; IM, insect meal diet; DID, distal intestine digesta; DIM, distal intestine mucosa.

989 <sup>1</sup>Monte Carlo *p* value.

990 <sup>2</sup>Phylogenetic isometric log-ratio transformed Euclidean distance.

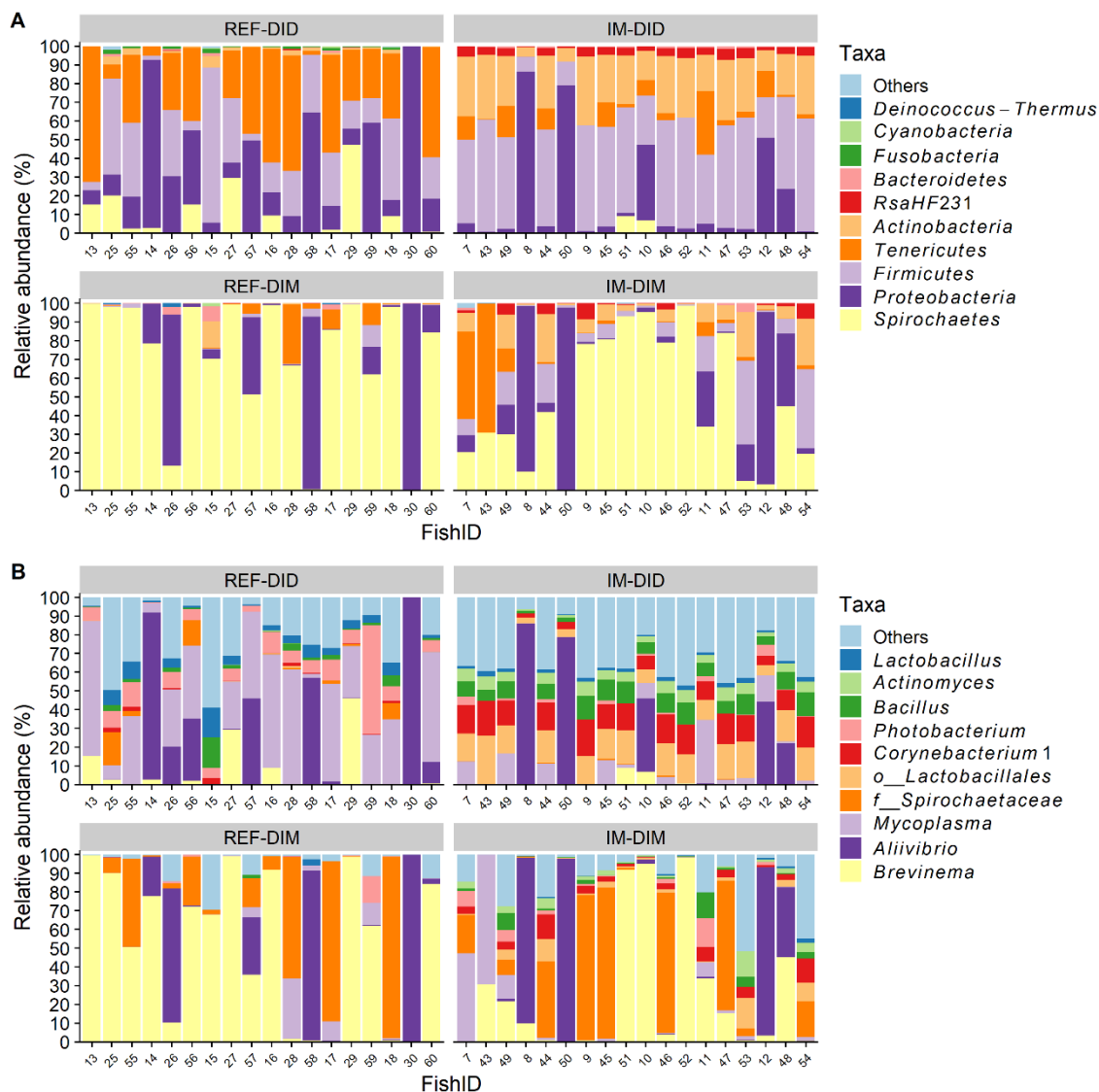
991 **Table 2. Test of homogeneity of multivariate dispersions among groups.**

Distance matrix	Conditional contrasts			
	REF-DID	REF-DIM	REF-DID	IM-DID
	VS. IM-DID	VS. IM-DIM	VS. REF-DIM	VS. IM-DIM
Jaccard	0.002	0.087	0.045	0.002
Unweighted UniFrac	0.002	0.711	0.200	0.002
Aitchison	0.453	0.046	0.046	0.369
PHILR (Euclidean) <sup>1</sup>	0.240	0.266	0.240	0.266

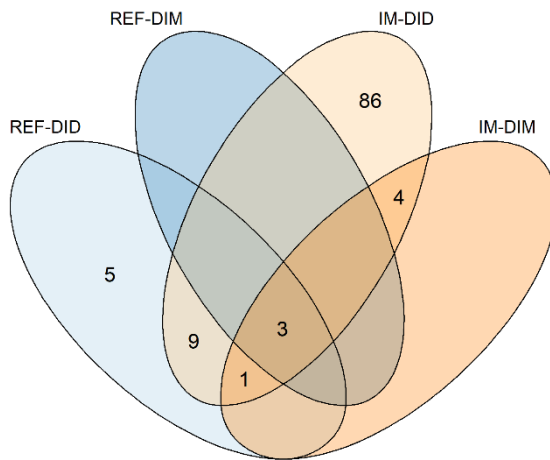
992 REF, reference diet; IM, insect meal diet; DID, distal intestine digesta; DIM, distal intestine mucosa.

993 <sup>1</sup>Phylogenetic isometric log-ratio transformed Euclidean distance.

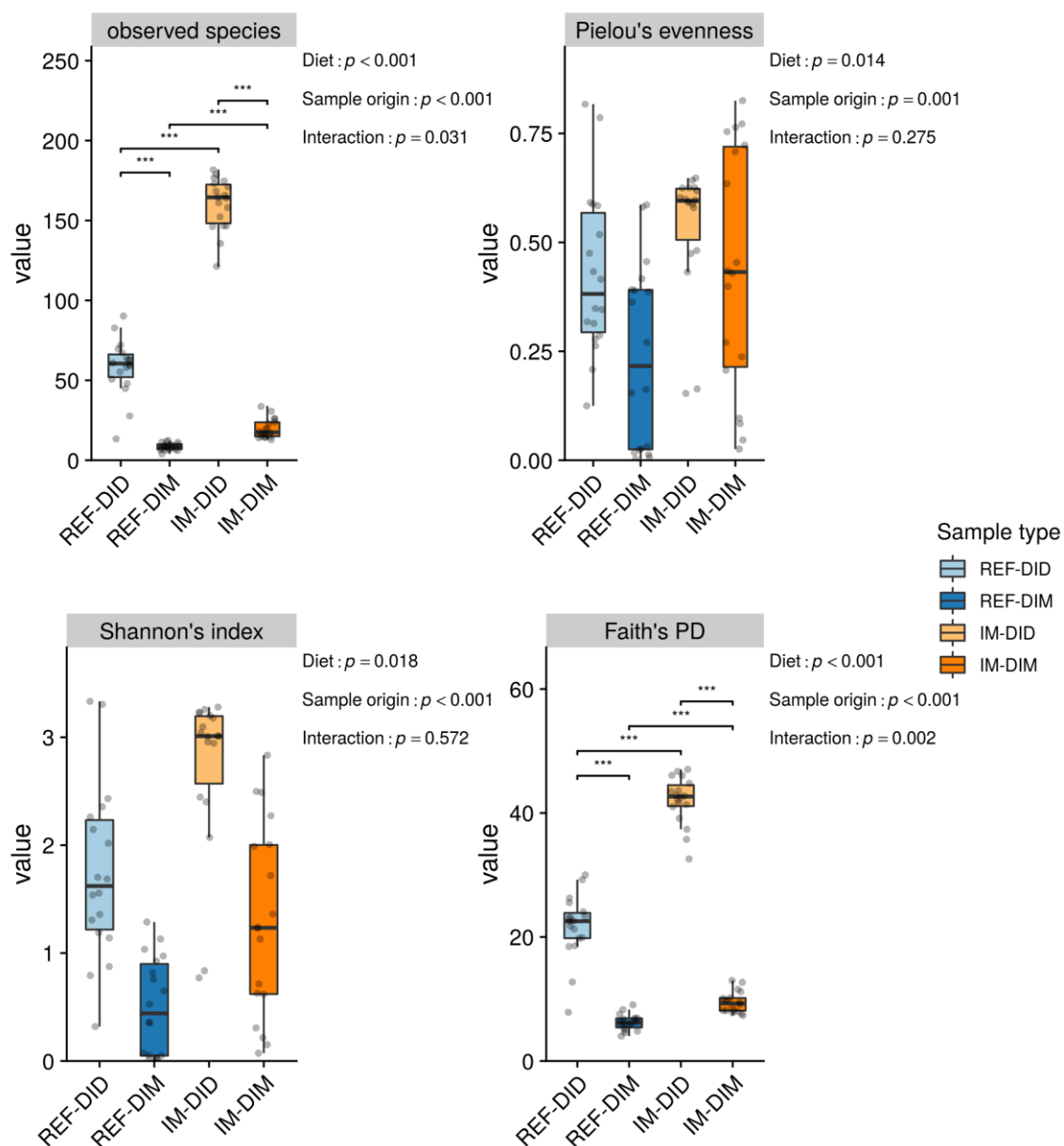
994 **Figures**



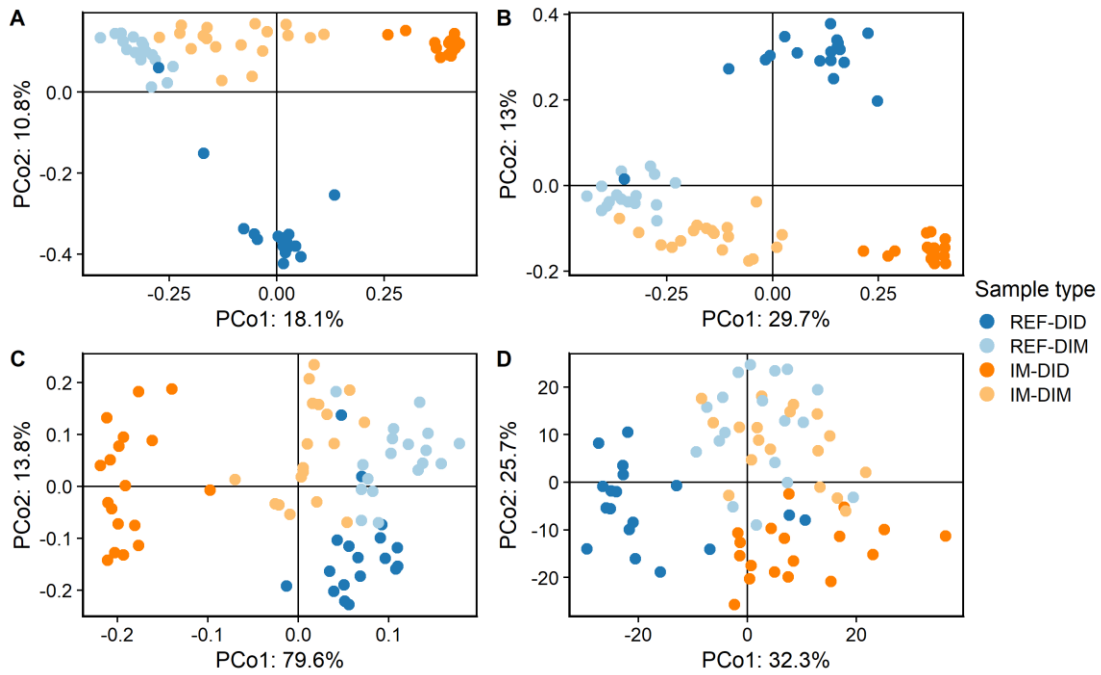
995 **Figure 1. Top 10 most abundant taxa of all samples at phylum (A) and genus (B)**  
 996 **level.** The samples are grouped by the sample type. *o*\_\_, order; *f*\_\_, family; REF, reference  
 997 diet; IM, insect meal diet; DID, distal intestine digesta; DIM, distal intestine mucosa.



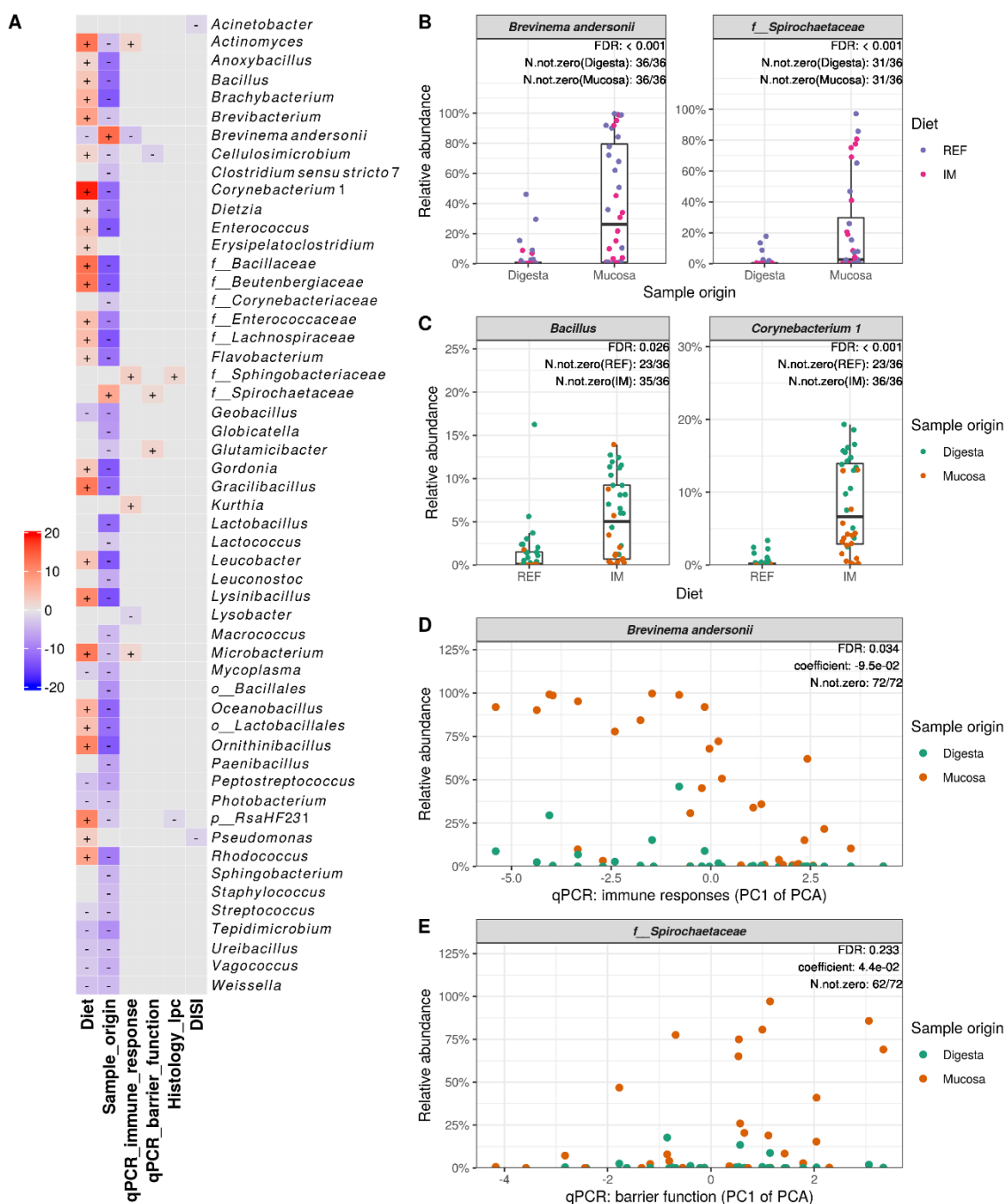
998 **Figure 2. Venn's diagram showing the shared and unique core microbiota in each**  
999 **sample type.** The core microbiota was computed using a prevalence threshold of 80%.  
1000 REF, reference diet; IM, insect meal diet; DID, distal intestine digesta; DIM, distal  
1001 intestine mucosa.



1002 **Figure 3. The sample origin and diet effects on the alpha-diversity of distal intestinal**  
 1003 **microbiota in seawater phase Atlantic salmon.** The  $p$  value of the main effects and their  
 1004 interaction are displayed on the top-right corner of each sub-plot. Asterisks denote  
 1005 statistically significant differences (\*,  $p < 0.05$ ; \*\*,  $p < 0.01$ ; \*\*\*,  $p < 0.001$ ). PD,  
 1006 phylogenetic diversity; REF, reference diet; IM, insect meal diet; DID, distal intestine  
 1007 digesta; DIM, distal intestine mucosa.



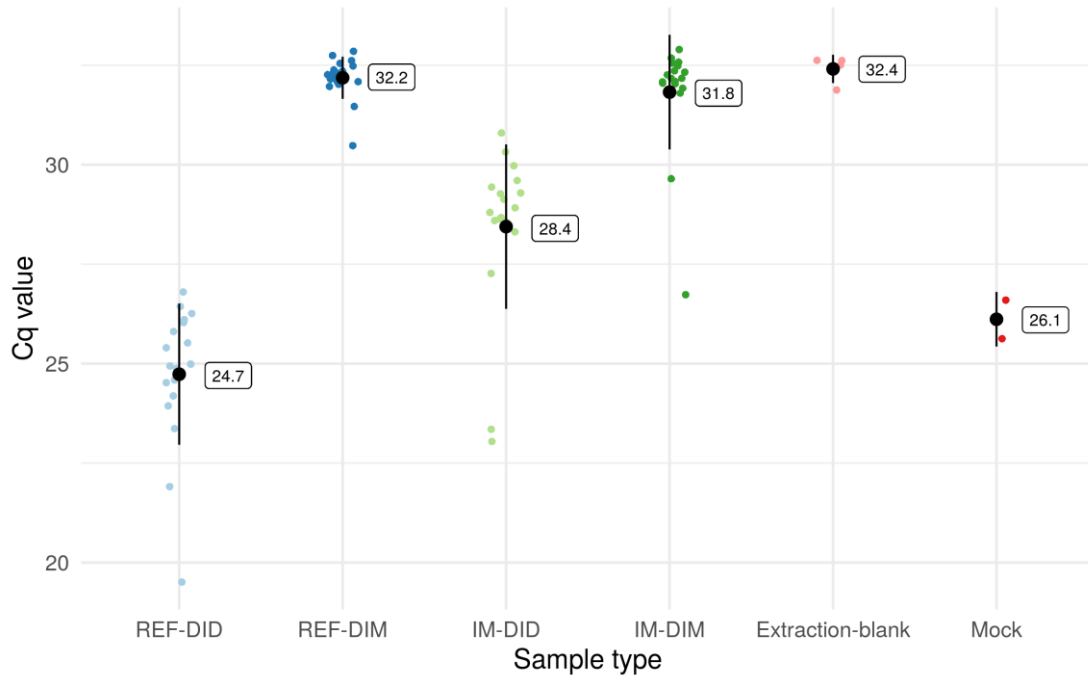
1008 **Figure 4. The sample origin and diet effects on the beta-diversity of distal intestinal**  
1009 **microbiota in seawater phase Atlantic salmon.** The PCoA plots were built on Jaccard  
1010 (A), unweighted UniFrac (B), Aitchison (C) and phylogenetic isometric log-ratio (PHILR)  
1011 transformed Euclidean (D) distance matrix, respectively. PCo, principle coordinate; REF,  
1012 reference diet; IM, insect meal diet; DID, distal intestine digesta; DIM, distal intestine  
1013 mucosa.



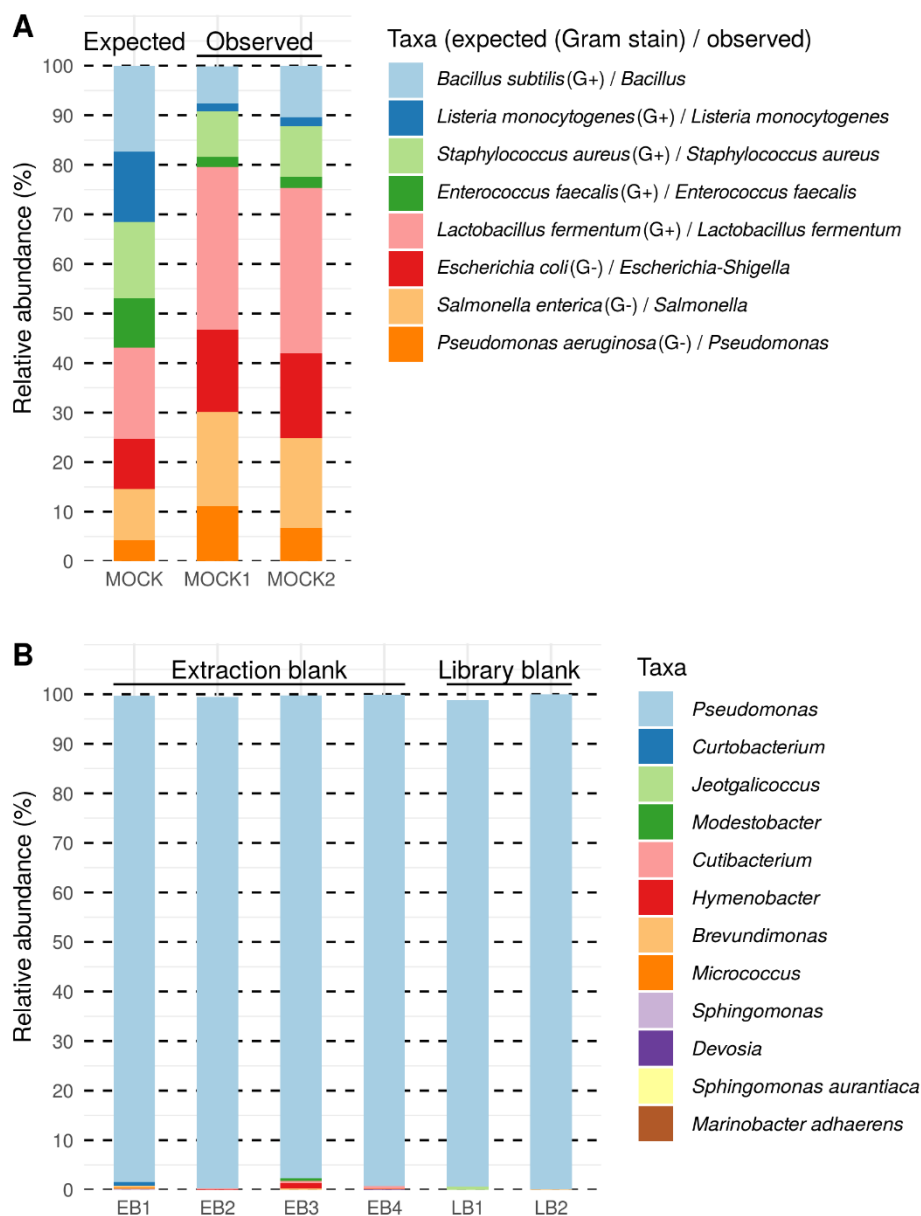
1014 **Figure 5. Significant associations between microbial clades and sample metadata. (A)**  
 1015 Heatmap summarizing all the significant associations between microbial clades and  
 1016 sample metadata. Color key:  $-\log(q\text{-value}) * \text{sign}(\text{coefficient})$ . Cells that denote  
 1017 significant associations are colored (red or blue) and overlaid with a plus (+) or minus (-)  
 1018 sign that indicates the direction of association: Diet (+), higher abundance in salmon fed  
 1019 the IM diet; Sample\_origin (+), higher abundance in mucosa samples; Histology\_lpc (+),

1020 higher abundance in salmon scored abnormal regarding lamina propria cellularity (lpc) in  
1021 the distal intestine; DISI (+), positive correlation between microbial clade abundance and  
1022 distal intestine somatic index (DISI); qPCR\_immune\_response (+) /  
1023 qPCR\_barrier\_function (+), negative correlation between microbial clade abundance and  
1024 the gene expression levels. (B) Taxa that are more abundant in the intestinal mucosa than  
1025 the digesta. (C) Representative taxa showing increased relative abundances in both  
1026 intestinal digesta and mucosa of salmon fed the IM diet. (D) The positive correlation  
1027 between the relative abundance of *B. andersonii* and immune gene expression levels in  
1028 the distal intestine. Note that the expression levels of the immune genes decreased as the  
1029 PC1 of the PCA increased. (E) The negative correlation between the relative abundance  
1030 of the unclassified *Spirochaetaceae* and the expression levels of barrier function relevant  
1031 genes. Also note that the expression levels of the barrier function relevant genes decreased  
1032 as the PC1 of the PCA increased. *p*\_\_, phylum; *o*\_\_, order; *f*\_\_, family; FDR, false  
1033 discovery rate; N.not.zero, number of observations that are not zero; REF, reference diet;  
1034 IM, insect meal diet.

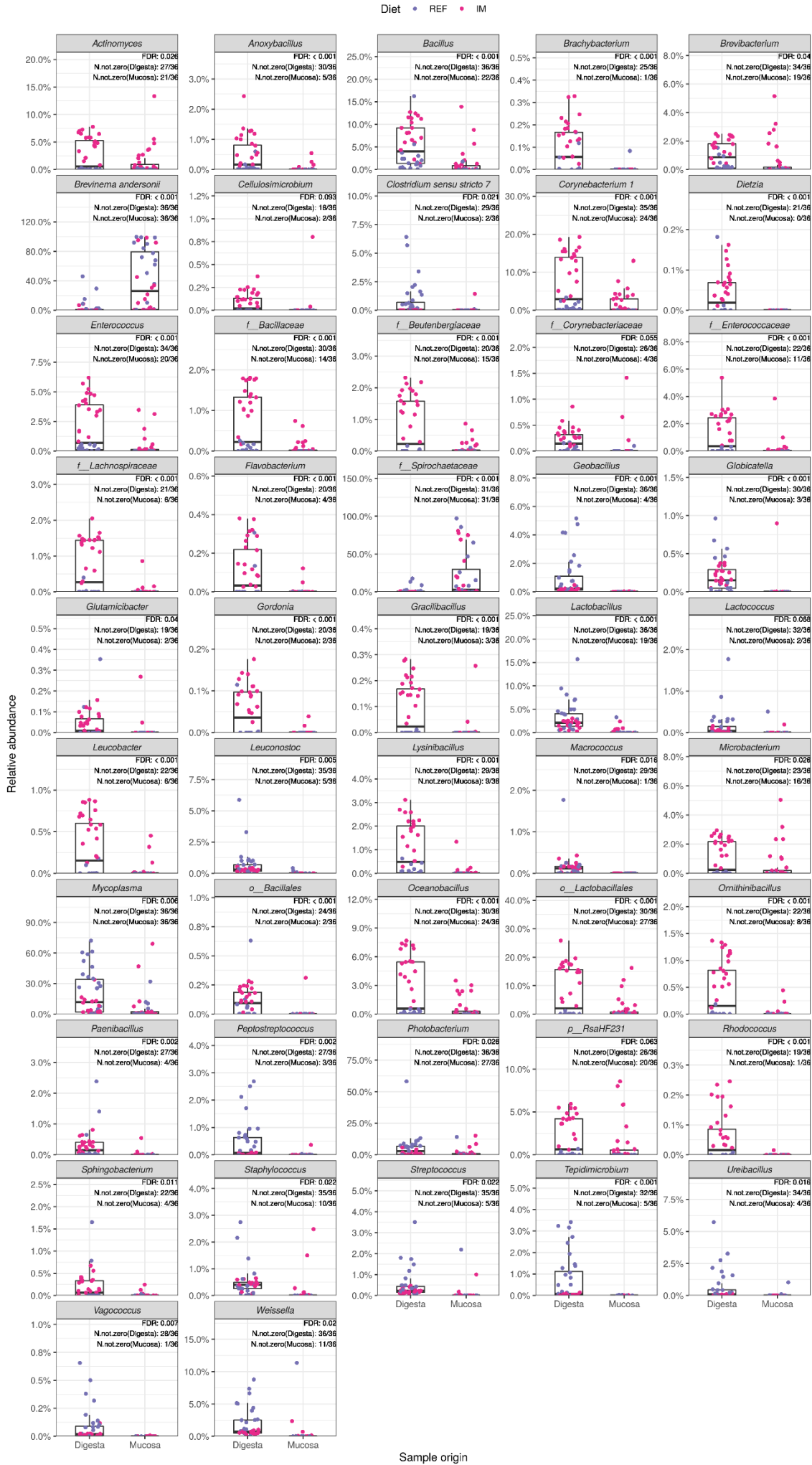
1035 **Supplemental figures**



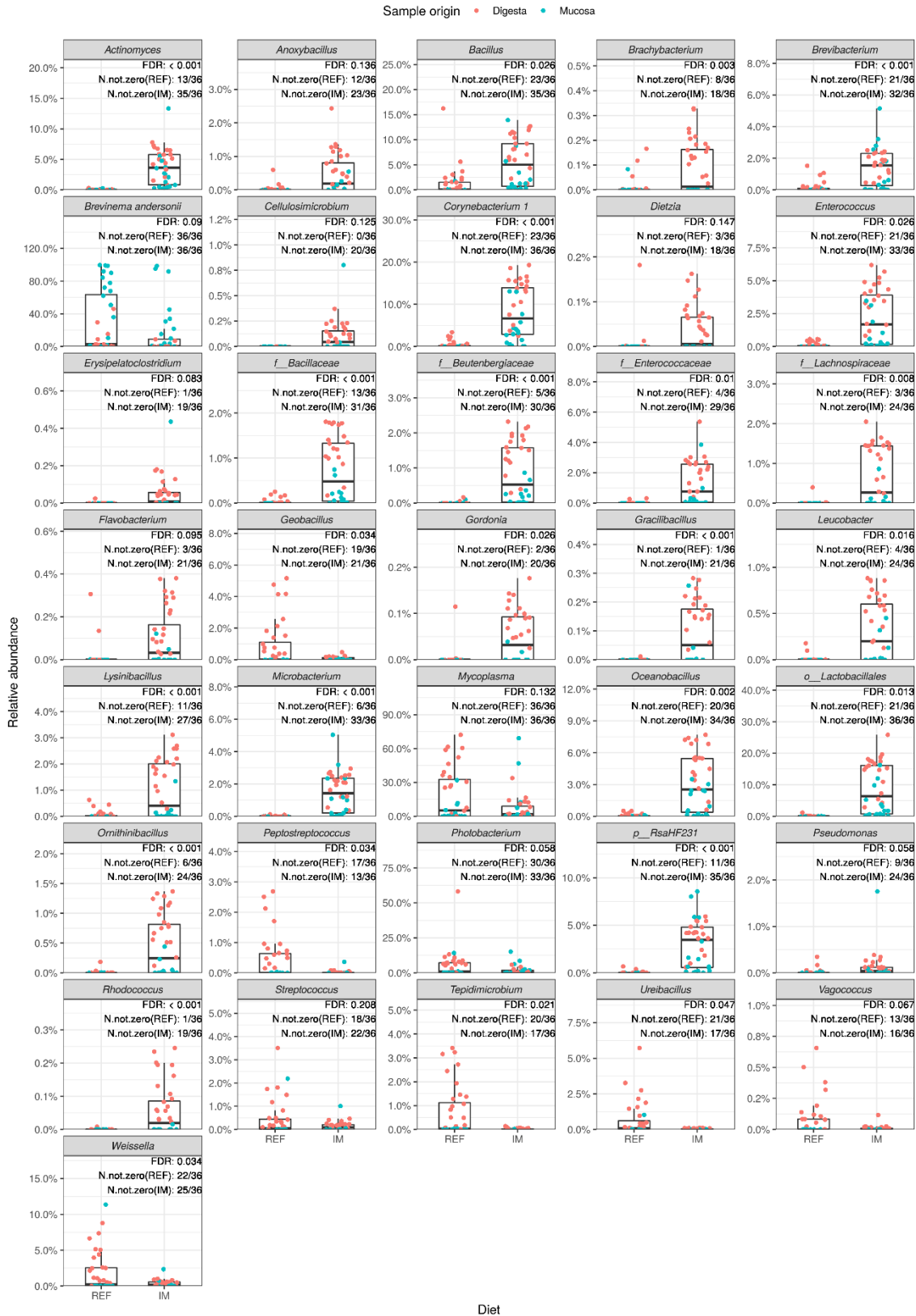
1036 **Figure S1. Quantification of bacterial 16S rRNA gene in different sample types using**  
1037 **qPCR.** Since the Cq values of most mucosa-associated samples were out of the linear  
1038 range of the standard curve, the Cq value was used as a proxy of 16S rRNA gene quantity  
1039 which is reliable for the screening of contaminant sequences. Data are presented as mean  
1040  $\pm$  1 standard deviation overlaying the raw data points. Abbreviations: REF, reference diet;  
1041 IM, insect meal diet; DID, distal intestine digesta; DIM, distal intestine mucosa.



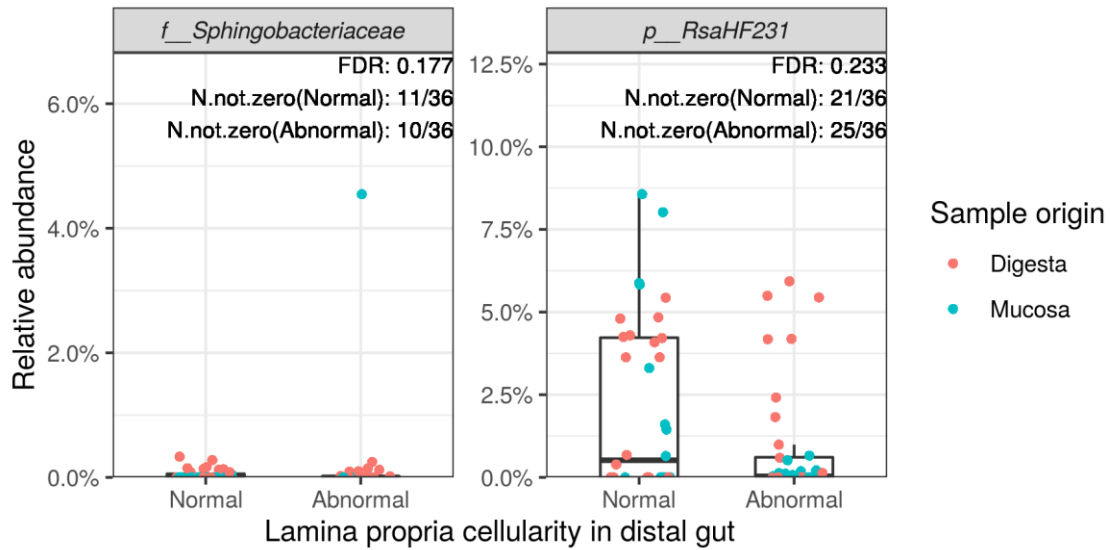
1042 **Figure S2. Taxonomic profile of the mock (A) and contaminating features in the**  
 1043 **negative controls (B).** The lowest level of taxonomic ranks was displayed for each taxon.  
 1044 EB, extraction blank; LB, library blank.



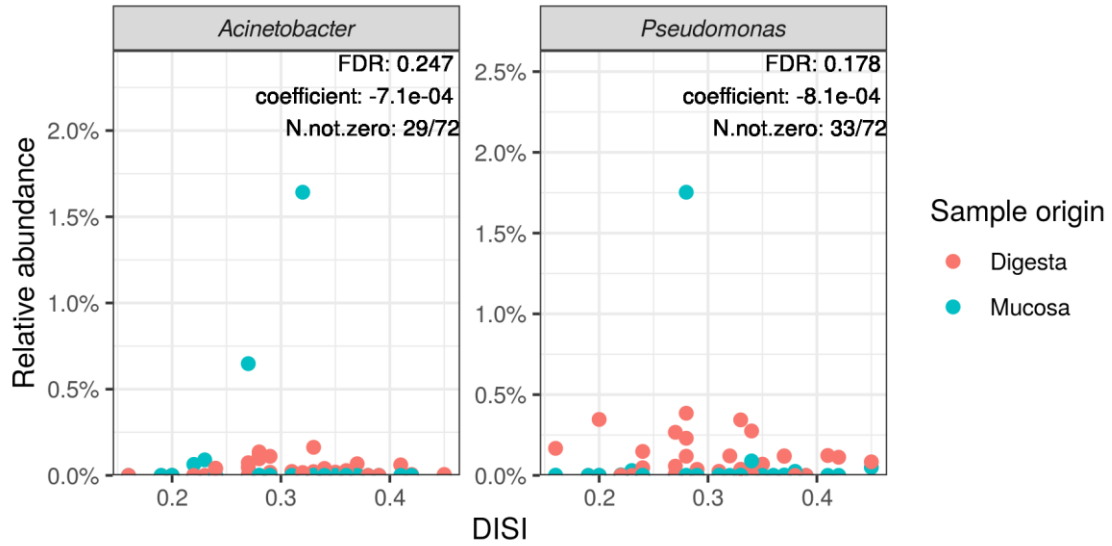
1045 **Figure S3. Microbial clades showing significant associations with sample origin.**  $p$  \_\_,  
 1046 phylum;  $o$  \_\_, order;  $f$  \_\_, family; FDR, false discovery rate; N.not.zero, number of non-  
 1047 zero observations; REF, reference diet; IM, insect meal diet.



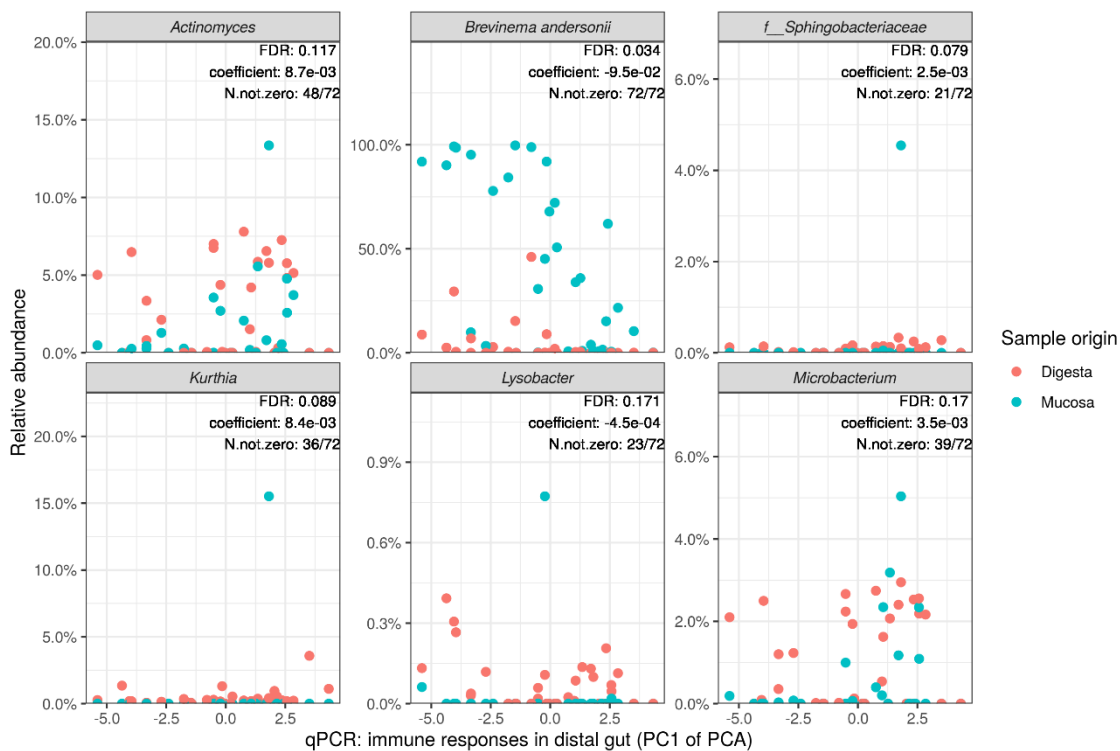
1048 **Figure S4. Microbial clades showing significant associations with diet.** *p*\_\_, phylum;  
 1049 *o*\_\_, order; *f*\_\_, family; FDR, false discovery rate; N.not.zero, number of non-zero  
 1050 observations; REF, reference diet; IM, insect meal diet.



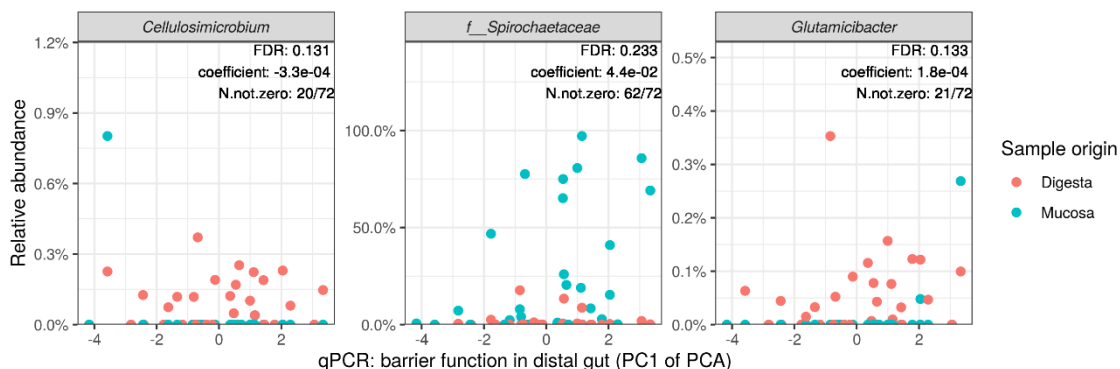
1051 **Figure S5. Microbial clades showing significant associations with histological scores**  
1052 **on lamina propria cellularity in the distal intestine.** *p\_\_*, phylum; *f\_\_*, family; FDR,  
1053 false discovery rate; N.not.zero, number of non-zero observations.



1054 **Figure S6. Microbial clades showing significant associations with distal intestine**  
1055 **somatic index (DISI).** FDR, false discovery rate; N.not.zero, number of non-zero  
1056 observations.



1057 **Figure S7. Microbial clades showing significant associations with immune gene**  
1058 **expressions in the distal intestine.** Since the expression levels of immune genes were  
1059 highly correlated, we ran a principle component analysis (PCA) and used the first  
1060 principle component (PC1) for the association testing to avoid multicollinearity and  
1061 reduce the number of association testing. Note that the expression levels of immune genes  
1062 decrease as the PC1 increases from left to right. Hence, a positive correlation coefficient  
1063 denotes a negative association between the microbial clade and immune gene expressions,  
1064 and vice versa. *f\_\_*, family; FDR, false discovery rate; N.not.zero, number of non-zero  
1065 observations.



1066 **Figure S8. Microbial clades showing significant associations with expressions of**  
1067 **barrier function related genes in the distal intestine.** Since the expression levels of  
1068 barrier function related genes were highly correlated, we ran a principle component  
1069 analysis (PCA) and used the first principle component (PC1) for the association testing  
1070 to avoid multicollinearity and reduce the number of association testing. Note that the  
1071 expression levels of barrier function related genes decrease as the PC1 increases from left  
1072 to right. Hence, a positive correlation coefficient denotes a negative association between  
1073 the microbial clade and barrier function related gene expressions, and vice versa. *f*\_\_,  
1074 family; FDR, false discovery rate; N.not.zero, number of non-zero observations.